REPORT DOCUMENTATION PAGE

Form Approved
OMB No. 0704-0188

1. AGENCY USE ONLY (Leave Blank)	2. REPORT DATE	3. REPORT TYPE AND DATES COVERED
	May 1993	Final

4. TITLE AND SUBTITLE
Multistage Decision Feedback and Trellis-Based Multiuser Receivers for Convoluntionally Coded CDMA Systems

5. FUNDING NUMBERS

6. AUTHORS
T.R. Giallorenzi and S.G. Wilson

AFRL-SR-BL-TR-98-
0446

7. PERFORMING ORGANIZATION NAME(S) AND ADDRESS(ES)
University of Virginia

9. SPONSORING/MONITORING AGENCY NAME(S) AND ADDRESS(ES)
AFOSR/NI
110 Duncan Avenue, Room B-115
Bolling Air Force Base, DC 20332-8080

10. SPONSORING/MONITORING AGENCY REPORT NUMBER

11. SUPPLEMENTARY NOTES

12a. DISTRIBUTION AVAILABILITY STATEMENT
Approved for Public Release

12b. DISTRIBUTION CODE

13. ABSTRACT *(Maximum 200 words)*
See attached.

14. SUBJECT TERMS	15. NUMBER OF PAGES
	16. PRICE CODE

17. SECURITY CLASSIFICATION OF REPORT	18. SECURITY CLASSIFICATION OF THIS PAGE	19. SECURITY CLASSIFICATION OF ABSTRACT	20. LIMITATION OF ABSTRACT
Unclassified	Unclassified	Unclassified	UL

A Technical Report

Multistage Decision Feedback and Trellis-Based Multiuser Receivers for Convolutionally Coded CDMA Systems

T.R. Giallorenzi
and
S.G. Wilson

SEAS Report No. UVA/538341/EE93/102
May 1993

Communications Systems Laboratory
DEPARTMENT OF ELECTRICAL ENGINEERING

SCHOOL OF
ENGINEERING
& APPLIED SCIENCE

University of Virginia
Thornton Hall
Charlottesville, VA 22903

UNIVERSITY OF VIRGINIA
School of Engineering and Applied Science

The University of Virginia's School of Engineering and Applied Science has an undergraduate enrollment of approximately 1,500 students with a graduate enrollment of approximately 600. There are 160 faculty members, a majority of whom conduct research in addition to teaching.

Research is a vital part of the educational program and interests parallel academic specialties. These range from the classical engineering disciplines of Chemical, Civil, Electrical, and Mechanical and Aerospace to newer, more specialized fields of Applied Mechanics, Biomedical Engineering, Systems Engineering, Materials Science, Nuclear Engineering and Engineering Physics, Applied Mathematics and Computer Science. Within these disciplines there are well equipped laboratories for conducting highly specialized research. All departments offer the doctorate; Biomedical and Materials Science grant only graduate degrees. In addition, courses in the humanities are offered within the School.

The University of Virginia (which includes approximately 2,000 faculty and a total of full-time student enrollment of about 17,000), also offers professional degrees under the schools of Architecture, Law, Medicine, Nursing, Commerce, Business Administration, and Education. In addition, the College of Arts and Sciences houses departments of Mathematics, Physics, Chemistry and others relevant to the engineering research program. The School of Engineering and Applied Science is an integral part of this University community which provides opportunities for interdisciplinary work in pursuit of the basic goals of education, research, and public service.

A Technical Report

Multistage Decision Feedback and Trellis-Based Multiuser Receivers for Convolutionally Coded CDMA Systems

T.R. Giallorenzi
and
S.G. Wilson

(804) 924-6111
(804) 924-6091
trg4d@virginia.edu
sgw@virginia.edu

Communications Systems Laboratory
Department of Electrical Engineering
SCHOOL OF ENGINEERING AND APPLIED SCIENCE
UNIVERSITY OF VIRGINIA
CHARLOTTESVILLE, VIRGINIA

SEAS Report No. UVA/538341/EE93/102 Copy No. 18
May 1993

Abstract

In this report, multistage decision feedback and trellis-based multiuser receivers are studied for convolutionally coded CDMA links. Some of the receiver structures proposed combine the functions of equalization and decoding while some consider the operations separately. A variety of decision feedback approaches are proposed, and through simulations, it is shown that these approaches are able to significantly outperform the conventional basestation architecture. Two trellis-based approaches are also proposed. The first is a partitioned structure which attacks the MUI equalization and decoding operations separately. The second approach is the maximum likelihood sequence estimator for this problem which is a combined equalizer and decoder. This decoder is formulated and its complexity is seen to depend exponentially on the number of users in the system, the number of states in the individual users' encoders and the number of input information bits per interval.

1. Introduction

In code division multiple access (CDMA) systems, multiple users transmit over a common communication channel, typically using the direct sequence spread spectrum technique. The receiver operating in this environment receives a signal which is the sum of all of the transmitted signals in noise, and the receiver's job is to reliably decode the signal of interest from this received composite signal. The users are not synchronized in general, and in addition, the received signal strengths of each user are typically unequal. Often, in an attempt to improve the performance of each link, error control coding will be used on each of the links as well. The receiver structures that will be studied in this paper may be for a base station in a cellular telephone cell or personal communication network (PCN) cell, or it may be for one of the user's receivers in a decentralized multiple access network of some kind.

The traditional method of coherently demodulating direct sequence CDMA signals is to synchronize a local code generator and oscillator to the signal of interest and then to make decisions on the received signal as though the desired signal is the only one present. The received signal usually consists of the desired signal, a multiuser interference (MUI) signal, thermal/shot noise and may be further degraded by dispersion. The traditional decoder's structure is that of a correlator or matched filter which is matched to the desired signal followed by a decoder if coding is used on the link.

The performance of the traditional decoder suffers for two major reasons. First, the signature sequences of the different users will not be orthogonal to each other, giving rise to the MUI, and second, in the common situation where all of the signals arriving at the receiver are of different strengths the strong signals tend to overwhelm the weak signals, even with reasonably good signature sequences. This second problem is referred to as the *near–far* problem.

A major improvement over the traditional receiver can be achieved by viewing the MUI not as a random noise signal, but instead as a structured interferer. Because all of the signals making up the MUI in a CDMA network are generally of the same structure as the signal of interest, and because their signature sequences are generally known, it is possible to augment the standard receiver structure and exploit this knowledge of the MUI by estimating it and attempting to cancel it, or by jointly estimating the entire message. The augmentation required consists of additional synchronization circuitry to lock into some or all of the interfering signals, and then to use these additional statistics to estimate the MUI.

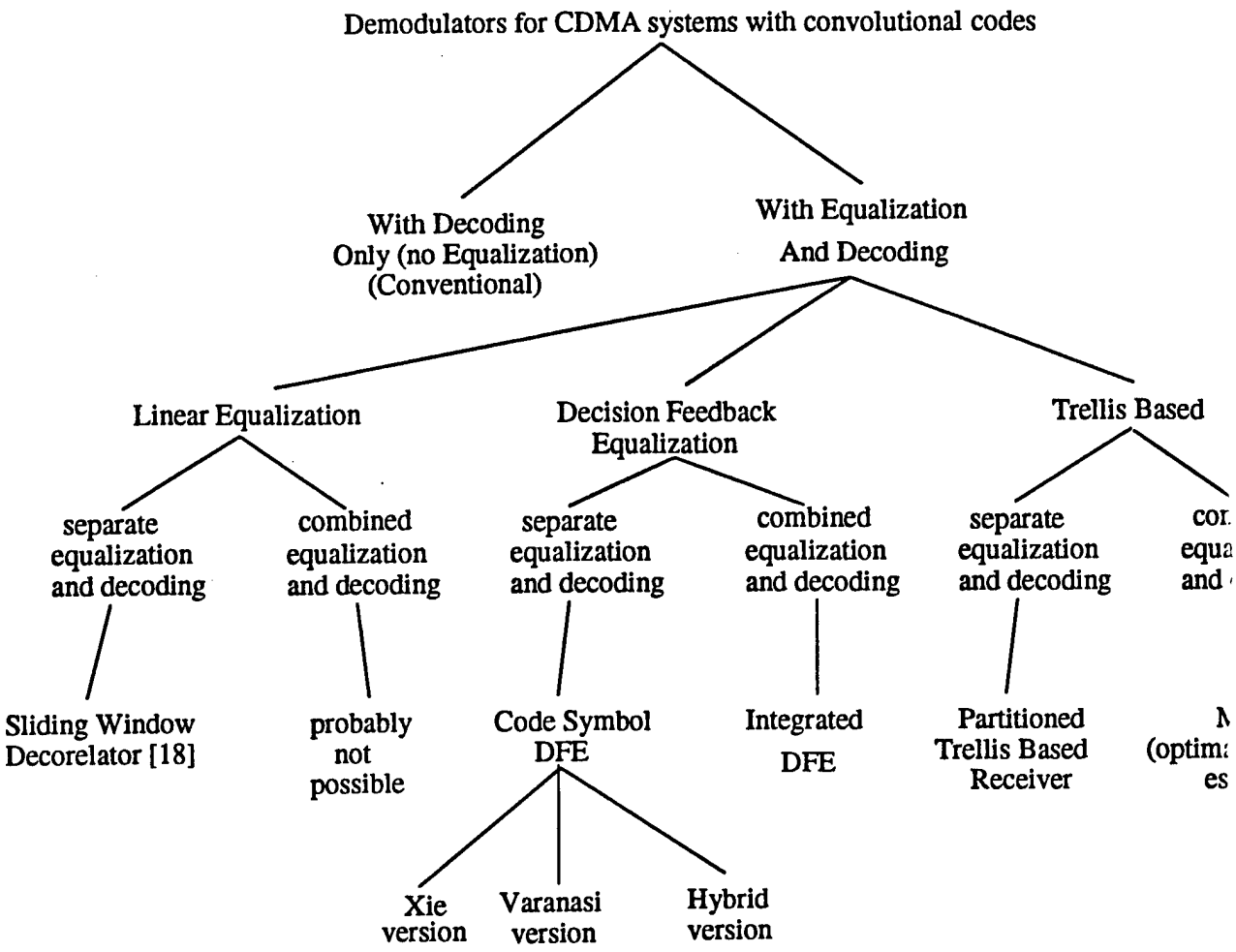

Figure 1: Tree diagram of the possible receiver structures for CDMA systems operating with convolutional

Two decoders will be proposed, a partitioned trellis-based receiver, which treats the equalization and decoding operations separately, and an optimum sequence estimator, which is the maximum likelihood sequence estimation receiver for this problem. The derivation of this optimal decoder and an analysis of its complexity and performance will constitute a large portion of this report.

2. Notation

It will be assumed that the CDMA system has K users operating on the same frequency in an asynchronous fashion. In general, it will be assumed that each user employs coding on its link. We will confine our attention to a particular form of coding, namely binary convolutional codes. The reason for this confinement of the scope of this work is primarily out of convenience. While it is quite conceivable that block codes could be used effectively on a CDMA link, convolutional codes have the advantage that they are stream codes, or operate in a sequential fashion. Because the decoders that will be studied in this work are sequential in nature, the convolutional codes are a much better match to the decoders than block codes. Also, in [16] it was shown that in CDMA systems, binary convolutional codes often outperform more general trellis codes which map information symbols onto M-level signals where M is larger than the alphabet size of the information symbols. In other words, there is no particular advantage to using nonbinary signals. This may be considered a further justification for the confinement in scope of this work to binary convolutional codes.

At each time interval, the convolutional code is generated for user k by passing P binary information bits, $\bar{I}_k(j) = (I_k(j),..., I_k(j-P+1))$, through a shift register consisting of W (P bit) stages and Q linear function generators, as shown in Figure 2. The input bits are shifted through the shift register P bits at a time, and the number of output bits for each P-bit input sequence is Q bits. The rate of the code is $R_c = P/Q$ and the constraint length of the code is W. The output sequence of code bits for the interval corresponding to input bits $\bar{I}_k(j)$ is $(D_k(n),...,D_k(n-Q+1))$. This output bit sequence is comprised of binary bits, as the linear function generators creating them will be assumed to be modulo-2 adders. Note that for $W = 1$ and $P = Q = 1$, we have the uncoded case, so in that case $D_k(n) = I_k(n)$.

In the time interval $[nT+\tau_k,(n+1)T+\tau_k)$, user k transmits data bit $D_k(n)$, where τ_k represents the time shift of the k^{th} user relative to some reference time, thus accounting for the asynchronism of the users relative to each other. T represents the time for one code bit duration and $T_b = QT/P$ is the information bit duration.

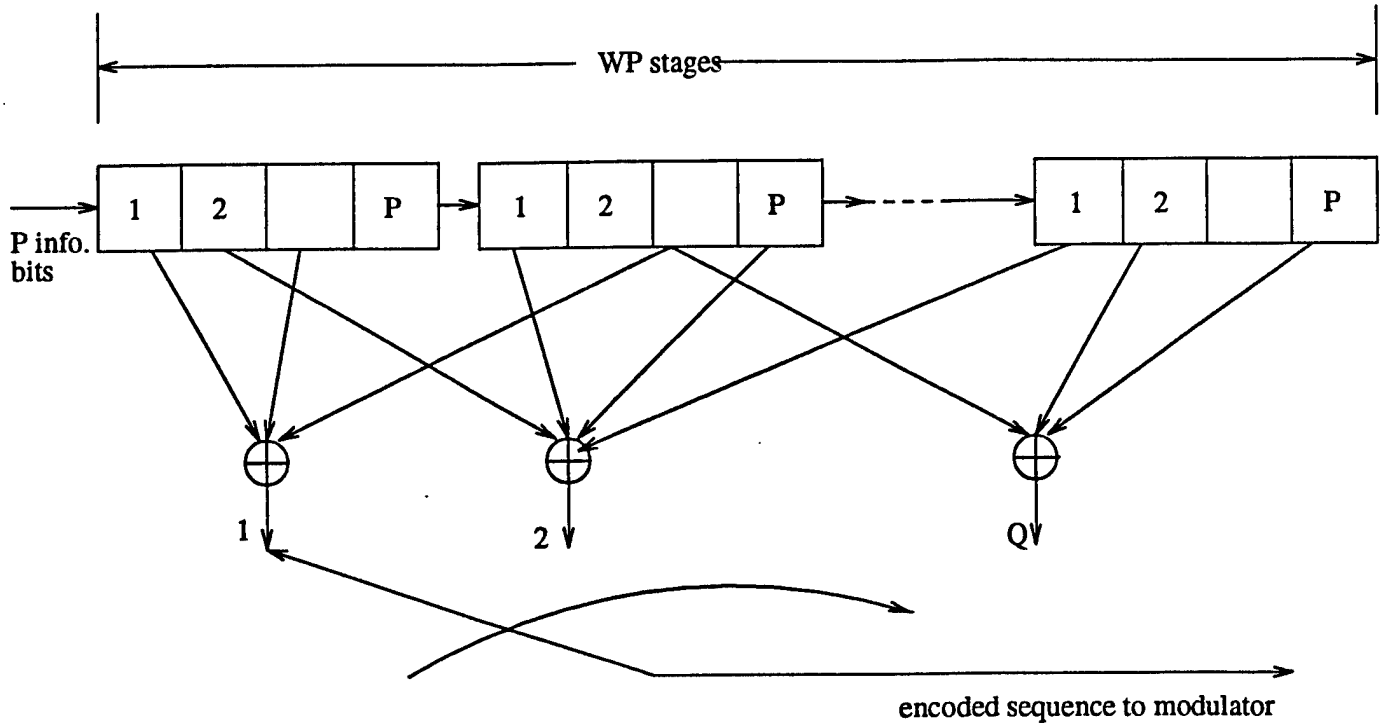

Figure 2 General convolutional encoder structure. [26]

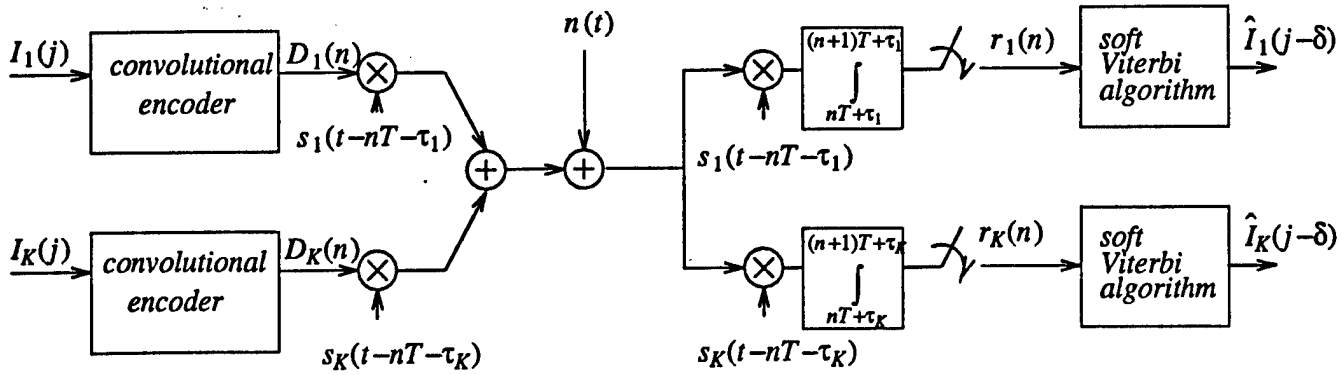

Figure 3 Convolutionally coded direct sequence CDMA link.
with a conventional basestation architecture. (case $E_j = 1$ shown)

Each user in the system is assigned a particular signature sequence, and it will be assumed that this signature sequence has a duration equal to the code bit interval, although this assumption can be relaxed with a change of the notation. We will combine the carrier and signature sequence into a single signal, thus the k^{th} carrier multiplied by the binary signature sequence, $PN_k(t)$, will be denoted by

$$s_k(t-nT-\tau_k) = \sqrt{2/T}\, PN_k(t-nT-\tau_k)\, cos\,(\omega_c(t-nT-\tau_k)) \qquad nT+\tau_k \le t \le (n+1)T+\tau_k \quad (1)$$

and it will have a time support limited to the time interval $[nT+\tau_k,(n+1)T+\tau_k)$. The energy of the k^{th} user's signal measured at the receiver will be denoted by E_k. It will be assumed that all K users transmit their signals through a common additive white Gaussian noise channel, and so the received signal will have the following form:

$$r(t) = \sum_{i=-\infty}^{\infty} \sum_{k=1}^{K} D_k(i)\sqrt{E_k}\; s_k(t-iT-\tau_k) + n(t)\ . \quad (2)$$

Next we define the partial cross-correlation of signature sequences j and k to be:

$$\rho_{jk}(i) = \int_{-\infty}^{\infty} s_j(t-\tau_j)\, s_k(t-iT-\tau_k)\, dt\ . \quad (3)$$

It is worth noting that $\rho_{jj}(0)=1$ and $\rho_{jk}(i)=\rho_{kj}(-i)$.

In section 4, we will derive a front end to the receiver which is appropriate for the maximum likelihood sequence estimator in that section, however, for now we assume that the front end to the receiver consists of a bank of K matched filters, each matched to one of the transmitted waveforms in the system. It was shown in [1] that the complete set of matched filter outputs generates sufficient statistics for the demodulation of each user's data. The output of the filter matched to the k^{th} signal at time $(i+1)T+\tau_k$ is

$$r_k(i) = \int_{iT+\tau_k}^{(i+1)T+\tau_k} r(t)\, s_k(t-iT-\tau_k)\, dt \quad (4)$$

where perfect synchronization has been assumed here between the k^{th} component of the received signal and the local signature sequence generator at the receiver. Substituting for $r(t)$ in equation (2) and integrating, we obtain

$$r_k(i) = \sum_{n=k+1}^{K} \rho_{kn}(-1)D_n(i-1)\sqrt{E_n} + \sum_{n=1}^{K} \rho_{kn}(0)D_n(i)\sqrt{E_n} + \sum_{n=1}^{k-1} \rho_{kn}(1)D_n(i+1)\sqrt{E_n} + n_k(i) \quad (5)$$

The base station that will be referred to as the conventional base station on a coded link is illustrated in Figure 3. In this figure, the component of the basestation which is attempting to estimate the j^{th} user's data operates with only the matched filter outputs for the j^{th} user. It will be assumed, as is shown in Figure 3, that the Viterbi algorithm

operating on each channel's observed code symbols is a soft-Viterbi algorithm operating with a decoding delay of δ information symbols. Note that generally δ will be several times the constraint length, W, of the code.

As in the uncoded case, there are a number of ways that a joint processor can operate to improve upon the performance of a conventional basestation. To this point, there has been some work on the analysis of the conventional basestation for the coded link problem, [16], but very little has been reported in the literature on the design of joint processors for coded links.

In [18] a sliding window version of the decorrelating detector, which was the linear decoder first proposed in [4], was studied and the authors alluded to the use of a convolutional code on the link. In that approach, a linear detector, whose decision statistic is a linear combination of the matched filter outputs, is used to equalize the MUI prior to decoding with the Viterbi algorithms. Results of this approach are not given, although they will undoubtably appear in a subsequent article.

Because the decision feedback approaches proved to be an attractive alternative in the uncoded case, (see [2], [3], [11] and [21]) due to their reasonable complexity and good performance, it is natural to begin by extending the decision feedback approaches to coded links. We will use the term decision feedback decoders in reference to the class of multistage decoders for the MUI equalization problem. This approach will be examined in section 3 of this report.

An obvious question with any system we wish to analyze is, "What is the optimal decoder's structure and performance?" Because the optimal sequence estimator for equalizing an uncoded CDMA system is a Viterbi algorithm, and because the Viterbi algorithm is also the optimal decoder for a single convolutionally coded link, it is reasonable to expect that the optimal sequence estimator for the coded link will also be a Viterbi algorithm operating on an appropriate trellis. It follows then, that trellis-based decoding techniques will be an appropriate and interesting class of decoders to study. In section 4, both a partitioned trellis-based approach and the optimum maximum likelihood sequence estimator will be derived. It will be shown that these decoders have an exponential complexity growth with K and W, and so this motivates our search for an effective suboptimum solution in the next section.

3. Decision Feedback Decoders for Coded Links

The most naive way in which decision feedback can be applied to a coded link is illustrated in Figure 4a. In this approach, termed the *hard code symbol DFE approach*,

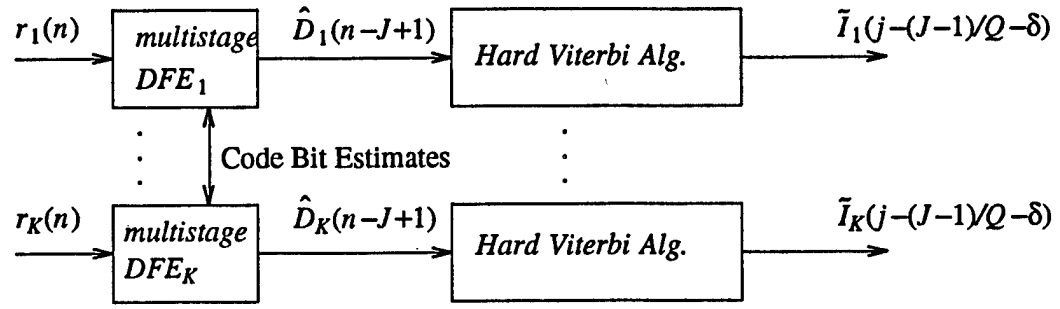

Figure 4a Hard code symbol DFE approach using a J-stage DFE on the code symbols.

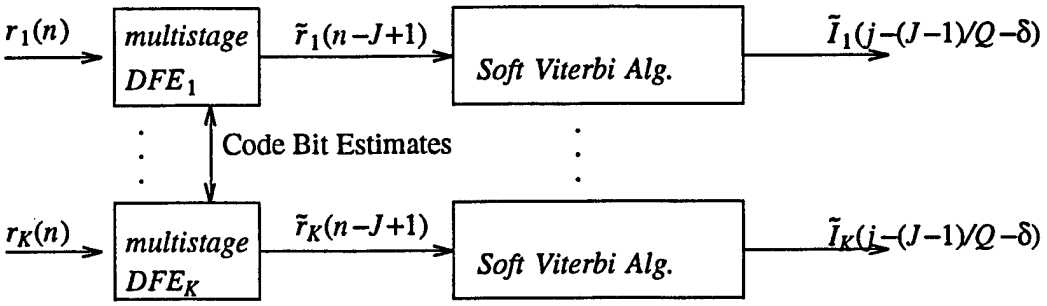

Figure 4b Soft code symbol DFE approach using a J-stage DFE on the code symbols with no hard decision in the final stage.

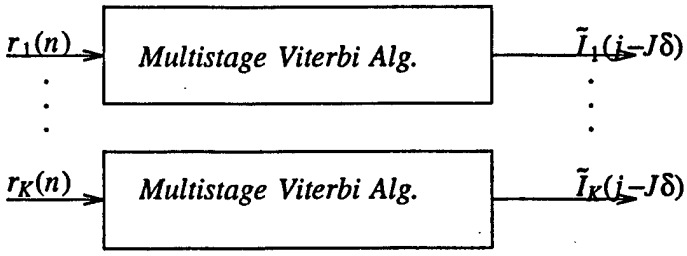

Figure 4c Integrated DFE with Viterbi algorithms operating at each stage of the DFE.

a DFE of some type jointly estimates the code bits and then feeds the results to a bank of hard-decision Viterbi decoders which use a Hamming distance metric.

A second approach, which will be called the *soft code symbol DFE approach* (SCS-DFE), is illustrated in Figure 4b. In this approach, again a multistage DFE operates on the set of matched filter outputs, by making tentative decisions and feeding these decisions back to make estimates of the MUI which will be subtracted from other matched filter outputs. The key difference in the SCS-DFE is that at the final stage, the MUI estimate will again be subtracted from the delayed matched filter output, but no hard-decision making will be performed. Instead, the modified matched filter output will be passed straight to the Viterbi decoder. This Viterbi decoder will be a soft-decision decoder and its metric will be a correlation-style metric as opposed to the Hamming distance metric of the hard-decision Viterbi decoder.

At this point, we have not committed to a particular type of multistage DFE. There have been at least three architectures proposed in the literature for asynchronous CDMA links, [2], [3], and [11], and there has also been some work on improving the decision making procedure of the algorithms, [21]. In [21], techniques such as the use of a decorrelator as the first stage decision maker, or a linear clipper or both were shown to provide gains in terms of the asymptotic multiuser efficiency for the two-user case. The improved decision making procedures in [21] can easily be applied to any of the three basic architectures. In this report, we will refer to the architecture in [2] as the Varanasi version, the architecture in [3] as the Xie version, and the architecture in [11] as the Hybrid version in keeping with the names used in [11].

All of these code symbol DFE approaches operate at the code symbol level as though there was no coding on the link, and then pass their decisions or improved statistics to an outer decoder. The problem with this approach is that the energy in each code symbol is less than that of each of the information symbols by a factor of R_c, the code rate. Furthermore, separating the functions of cancelling the MUI and decoding the message does not take full advantage of the coding on the link. The following approach attempts to alleviate these shortcomings.

The decision feedback equalizer illustrated schematically in Figure 4c, and more explicitly in Figure 5, will be called the *integrated DFE*. The idea in the integrated DFE is that the MUI can be more reliably estimated by exploiting the coding. In other words, instead of using a hard-decision device in the first stage of the DFE, we may decode the message using a soft-decision Viterbi algorithm operating on the stream of matched filter outputs in the j^{th} channel, and then re-encode the decoded bits to form estimates of the code bits. Due to the delay in the Viterbi decoder, the delay between stages and the

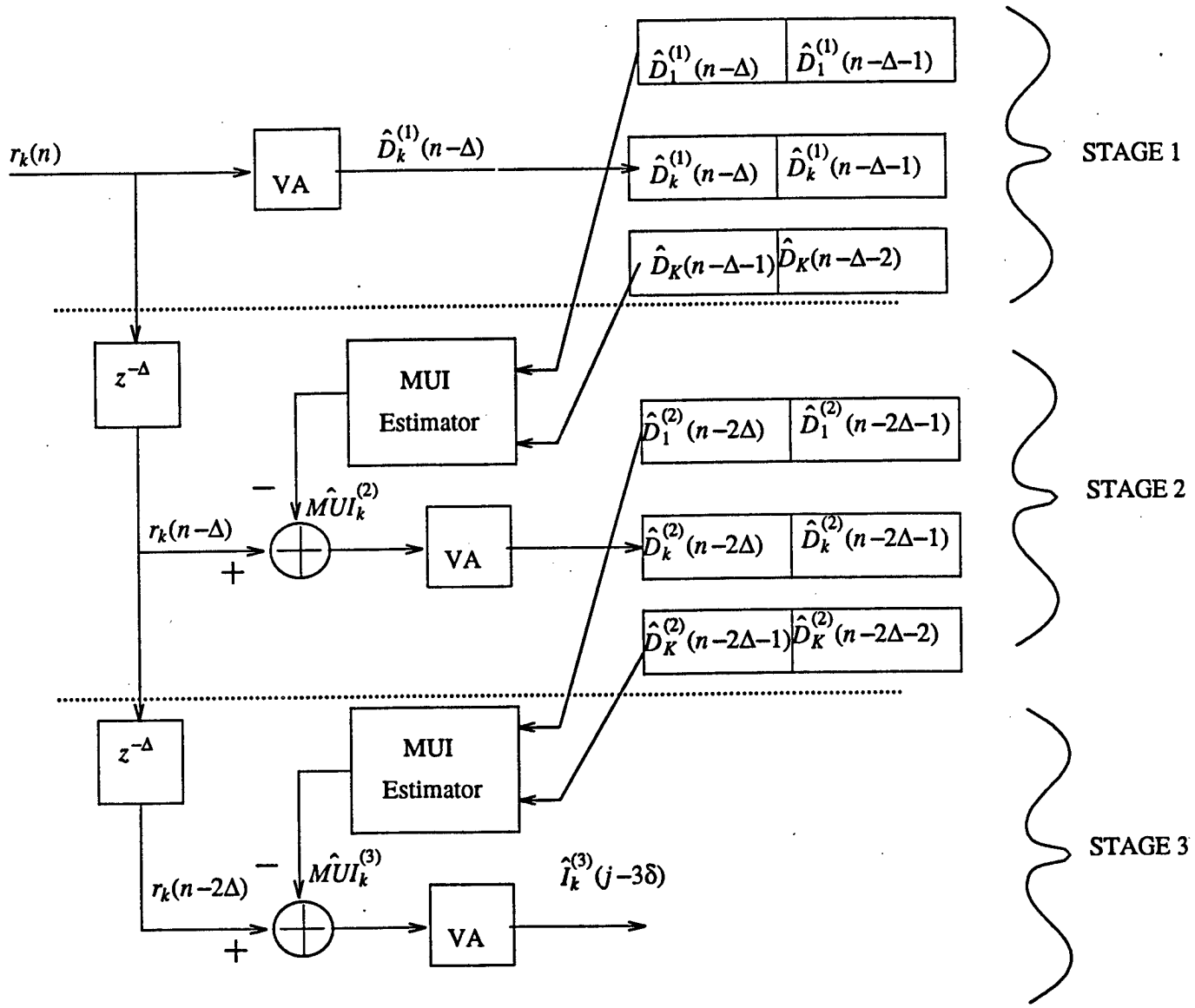

Figure 5 The structure of a 3-stage integrated DFE for the k^{th} user with Viterbi algorithms (denoted VA) at each stage. Δ is the maximum delay in code bit periods corresponding to δ information bit periods

buffering operations will be greater than in a code symbol DFE. In this DFE approach, at each stage, Viterbi decoders will replace the hard-decision comparators that were present in the code symbol multistage DFEs. Again, as in the uncoded case, the decision feedback may be performed for as many stages as is desired.

A characteristic of convolutional codes, or most codes for that matter, is that at very low signal to noise ratios, the coded link may perform worse than an uncoded link. When the signal to noise ratio is in this regime, it is possible that the Viterbi decoder whose outputs are re-encoded to form the ML estimate of the code bit sequence, may perform worse than a simple hard-decision device operating on the code bits without regard to the coding. As a result of this characteristic, it is important that the combination of the thermal noise and MUI is not so strong that the re-encoded Viterbi output sequence is worse than the estimated code bits of a simple threshold detector for the integrated DFE to outperform an SCS-DFE. Basically, the structure which provides better estimates of the code bit sequence will have a better estimate of the MUI in the other channel's multistage decoders. In general, because coding generally allows better estimates of the transmitted sequence, it is reasonable to expect the integrated DFE to outperform an SCS-DFE of a similar architecture.

The performance of this class of approaches is difficult to evaluate analytically, especially for more than two users, as in the uncoded case, [2], [3], and [11]. As a result, simulation will be the performance evaluation technique. Because the structure of the integrated DFE is most like the Varanasi style uncoded link multistage decoder, it is interesting to compare the integrated DFE with the Varanasi style SCS-DFE. In addition, because it was shown in [11] that in most cases, the Hybrid DFE outperforms the other two architectures on an uncoded link, it is an obvious candidate for use in an SCS-DFE structure. Thus, the structures that were simulated were the Hybrid and Varanasi versions of the SCS-DFE and the integrated DFE. The modifications to the decision making devices in each preliminary stage of the multistage decoders discussed in [21] were not considered here, although those modifications may provide improvements in some cases.

Figure 6 shows two sets of signature sequences for a four-user system (the complex envelopes of the signals are shown assuming a carrier phase of zero). The resulting crosscorrelation structure is also shown in this figure. There are many signature sets and delays, in general, which yield the same crosscorrelation structure, and so the signature sets which are shown are provided only to illustrate that the set of crosscorrelations simulated are achievable. (It is possible to construct correlation matrices which are not in the range of achievable values.) Both signature sets shown are constructed to provide a high level of MUI which is fairly balanced between the users. This choice of signature

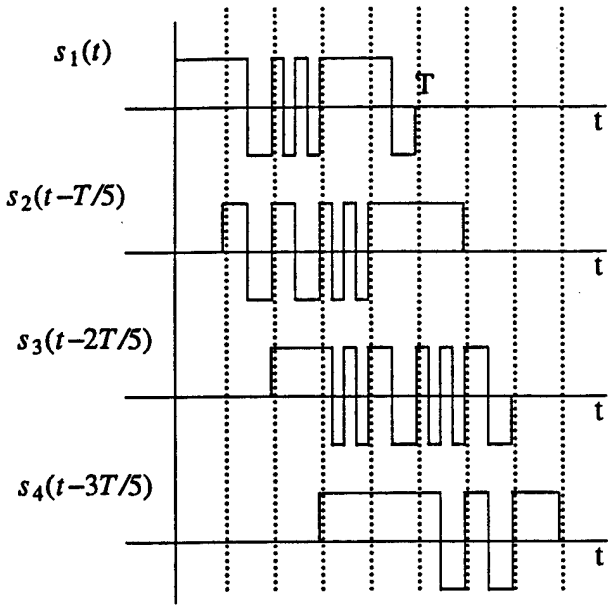

$$\begin{bmatrix} \rho_{11}(-1) & \rho_{12}(-1) & \rho_{13}(-1) & \rho_{14}(-1) \\ \rho_{21}(-1) & \rho_{22}(-1) & \rho_{23}(-1) & \rho_{24}(-1) \\ \rho_{31}(-1) & \rho_{32}(-1) & \rho_{33}(-1) & \rho_{34}(-1) \\ \rho_{41}(-1) & \rho_{42}(-1) & \rho_{43}(-1) & \rho_{44}(-1) \end{bmatrix} = \begin{bmatrix} 0 & .2 & .2 & .2 \\ 0 & 0 & .2 & .2 \\ 0 & 0 & 0 & .2 \\ 0 & 0 & 0 & 0 \end{bmatrix}$$

$$\begin{bmatrix} \rho_{11}(0) & \rho_{12}(0) & \rho_{13}(0) & \rho_{14}(0) \\ \rho_{21}(0) & \rho_{22}(0) & \rho_{23}(0) & \rho_{24}(0) \\ \rho_{31}(0) & \rho_{32}(0) & \rho_{33}(0) & \rho_{34}(0) \\ \rho_{41}(0) & \rho_{42}(0) & \rho_{43}(0) & \rho_{44}(0) \end{bmatrix} = \begin{bmatrix} 1 & .2 & .2 & .2 \\ .2 & 1 & .2 & .2 \\ .2 & .2 & 1 & .2 \\ .2 & .2 & .2 & 1 \end{bmatrix}$$

$$\rho_{jk}(1) = \rho_{kj}(-1)$$

Figure 6a An example set of signature waveforms and delays which yield the correlation structure shown.

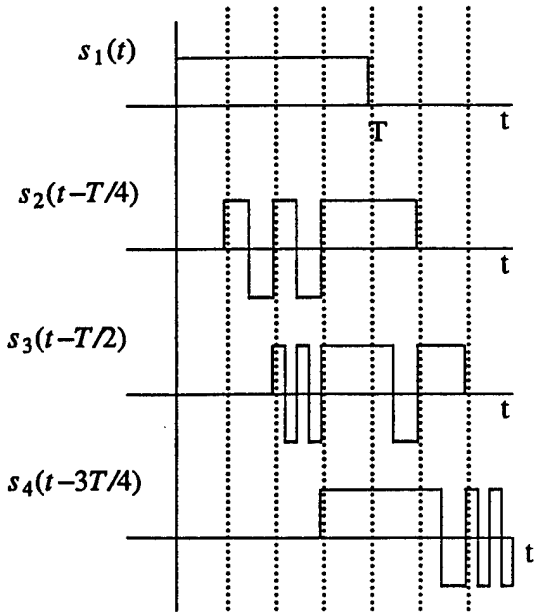

$$\begin{bmatrix} \rho_{11}(-1) & \rho_{12}(-1) & \rho_{13}(-1) & \rho_{14}(-1) \\ \rho_{21}(-1) & \rho_{22}(-1) & \rho_{23}(-1) & \rho_{24}(-1) \\ \rho_{31}(-1) & \rho_{32}(-1) & \rho_{33}(-1) & \rho_{34}(-1) \\ \rho_{41}(-1) & \rho_{42}(-1) & \rho_{43}(-1) & \rho_{44}(-1) \end{bmatrix} = \begin{bmatrix} 0 & .25 & .25 & .25 \\ 0 & 0 & 0 & .25 \\ 0 & 0 & 0 & .25 \\ 0 & 0 & 0 & 0 \end{bmatrix}$$

$$\begin{bmatrix} \rho_{11}(0) & \rho_{12}(0) & \rho_{13}(0) & \rho_{14}(0) \\ \rho_{21}(0) & \rho_{22}(0) & \rho_{23}(0) & \rho_{24}(0) \\ \rho_{31}(0) & \rho_{32}(0) & \rho_{33}(0) & \rho_{34}(0) \\ \rho_{41}(0) & \rho_{42}(0) & \rho_{43}(0) & \rho_{44}(0) \end{bmatrix} = \begin{bmatrix} 1 & .25 & .25 & .25 \\ .25 & 1 & .25 & .5 \\ .25 & .25 & 1 & .25 \\ .25 & .5 & .25 & 1 \end{bmatrix}$$

$$\rho_{jk}(1) = \rho_{kj}(-1)$$

Figure 6b A second set of signature waveforms and delays which yield the more severe correlation structure shown.

waveforms does not necessarily represent an intelligent choice of waveforms for this particular chip-to-symbol rate ratio. It is also probably safe to say that if the MUI was much more severe than that simulated in these examples, then the dominating problem would most likely be that of the initial acquisition of the local oscillators and code sequence generators at the front end of the receiver rather than the performance of the multiuser detectors if synchronization is achieved.

Figure 7 shows performance on the "0.2 channel" illustrated by Figure 6a. As Figure 7 illustrates, the conventional decoder suffers about a 3 dB loss at $P_b\,average = 2 \cdot 10^{-3}$ relative to the performance of the same receiver operating in the absence of MUI. In this environment, the integrated DFE is able to nearly recoup all of this loss, while the various SCS-DFEs are able to only recoup some of the loss. It may thus be concluded that the thermal noise and MUI are weak enough to be operating in the regime where a receiver which exploits the coding performs better than one which does not. The Hybrid version of the SCS-DFE outperforms the Varanasi version of the SCS-DFE which is similar to the results obtained on the uncoded link simulated in [11].

Figure 8 shows the performance on the more severe channel illustrated in Figure 6b. In this figure, it is evident that all of the decoders perform significantly worse than in the "0.2 channel" due to the more severe MUI. The integrated DFE still uniformly outperforms the Varanasi version of the SCS-DFE. For these particular channel characteristics, however, the hybrid SCS-DFE is able to outperform the integrated DFE at larger values of E_b/N_0. While this may seem surprizing at first, it is simply due to the fact that even though the hybrid SCS-DFE performs separate equalization and decoding, it has a high quality first stage which is able to provide better code symbol estimates to the second stage MUI estimator than the conventional Viterbi algorithm operating in the first stage of the integrated DFE. This case illustrates that when the MUI is strong enough, the integrated DFE will not always outperform a well designed SCS-DFE, although it does in most cases.

An additional key consideration in the choice of the receiver structure is complexity. The relative complexities of the various approaches may be estimated by considering the time complexity per bit. [1] This measure is, roughly speaking, the number of "metrics" which must be computed for each decided bit. In the DFE structures considered here, metrics are formally being computed in the Viterbi decoders, and there is some additional complexity associated with the MUI estimation procedure in the DFE part of the receivers. In general, the computation of the MUI in each stage of the DFE structures is roughly equivalent in complexity to the computation of one metric in the Viterbi decoder. Thus adopting this convention, we may conclude that a J-stage SCS-

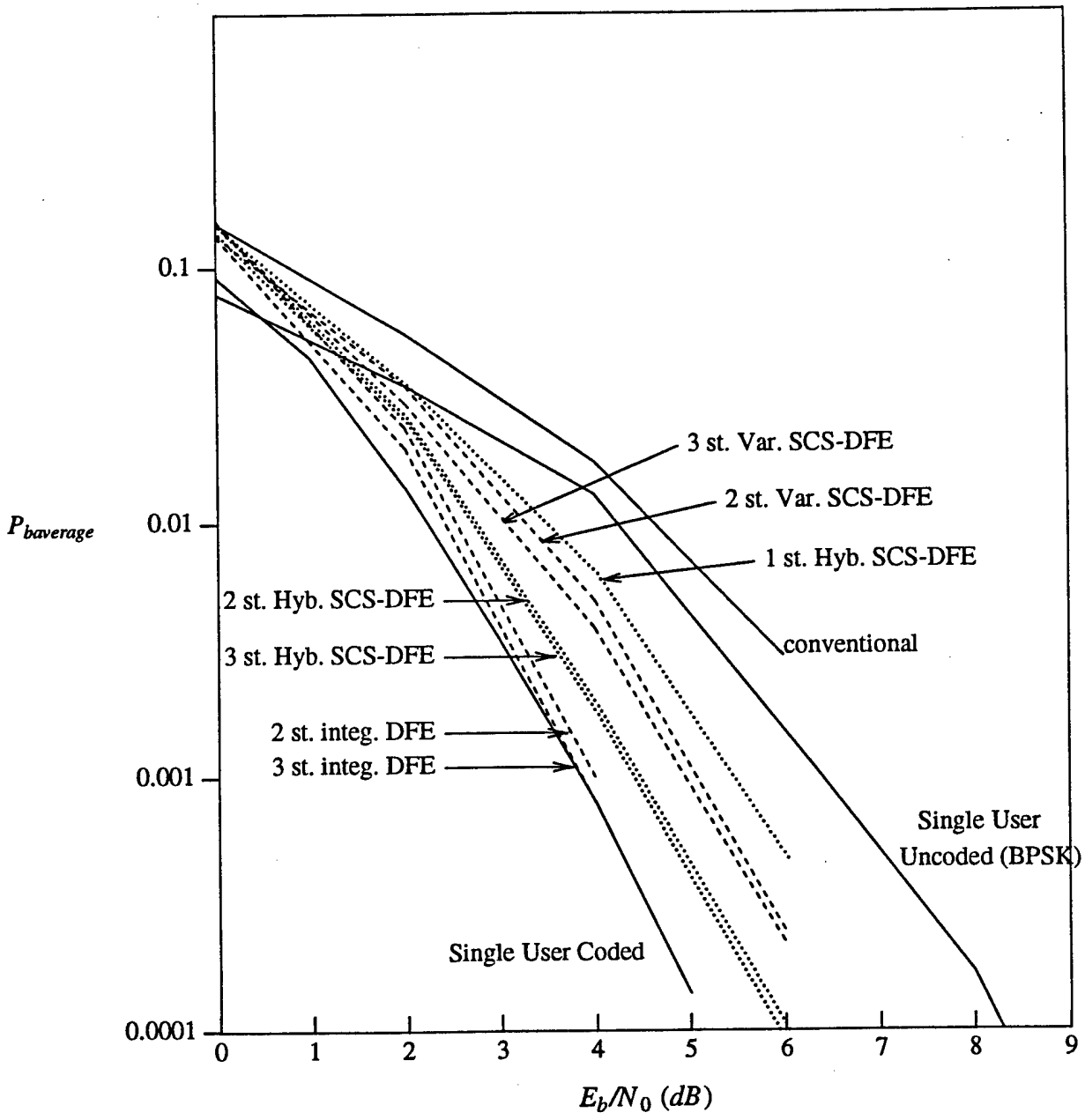

Figure 7 Performance curves of the various decision feedback receivers for the 4-user 0.2 channel illustrated in Figure 6a. The solid lines show a single user system (no MUI) with and without the rate-1/2 4-state convolutional code. Also shown are the one, two and three stage soft code symbol DFEs for both the Varanasi (dashed) and Hybrid (dotted) architectures, and a one, two and three stage integrated DFE (dashed lines). Note that the Varanasi style one-stage soft code symbol DFE and the one-stage integrated DFE are both equivalent to the conventional receiver.

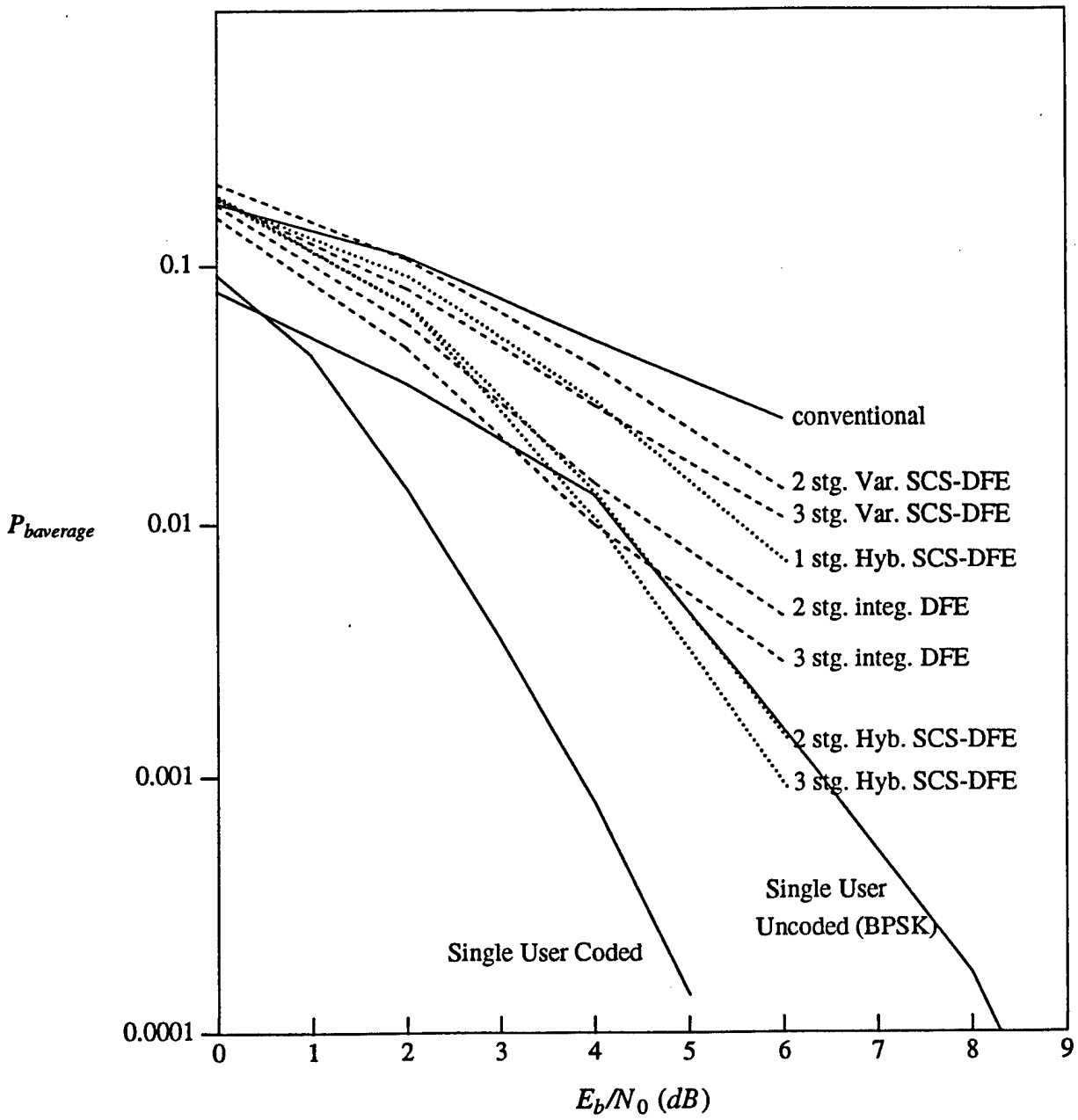

Figure 8 Performance curves of the various decision feedback receivers for the more severe 4-user 0.25 channel illustrated in Figure 6b. The solid lines show a single user system (no MUI) with and without the rate-1/2 4-state convolutional code. Also shown are the one, two and three stage soft code symbol DFEs of both the Varanasi (dashed) and Hybrid (dotted) architectures, and a one, two and three stage integrated DFE (dashed lines). Note that the Varanasi style one-stage soft code symbol DFE and the one-stage integrated DFE are both equivalent to the conventional receiver.

DFE operating on a link with rate $1/Q$ codes, for example, has a time complexity per decoded bit of roughly TCB = $O(JQ+2^W)$ where W is the constraint length of the code used. In contrast, the J-stage integrated DFE has a time complexity of roughly TCB = $O((J-1)Q+J2^W)$, which is significantly higher than that of the SCS-DFE, although it is far less than that of the trellis-based approaches which will be studied in section 4 of this report.

In the general rate P/Q code case, if $\kappa = \log_2 S$ where S is the number of states in each user's encoder, then κ represents the total binary memory order of each user's encoder. Using this definition, it is not difficult to determine the TCB for this general case. The SCS-DFE has a TCB = $O([JQ+2^{\kappa+P}]/P)$ and the integrated DFE has TCB = $O([(J-1)Q+J2^{\kappa+P}]/P)$.

Another consideration in the choice of receiver structures may be the delay between the observation of the matched filter output corresponding to a particular information bit and the ultimate estimation of that bit. If it is assumed that the Viterbi decoders used operate with a decoding delay of δ information symbols, which is typically on the order of $5W$, then the overall decoding delay of the J-stage SCS-DFE is $(J-1)/Q+\delta \approx J+5W$. The corresponding decoding delay of the J-stage integrated DFE is roughly $J\delta \approx 5JW$.

We may thus conclude that the integrated DFE has a larger TCB, and a longer decoding delay than any of the SCS-DFE approaches, but its performance is better in most cases. As a result, the appropriate choice of receiver configuration will depend on the expected severity of the channel and the complexity and delay constraints on the receiver. As we have seen in Figure 8, however, even the integrated DFE does not perform well when the MUI becomes too strong. As a result, it is natural to look for nearly optimal and optimal receiver structures which do perform well even in these severe cases. The other motivation for looking to the nearly optimal and optimal schemes is to provide a benchmark for comparison with the suboptimal DFE schemes in all cases. This will allow us to see how close the suboptimal approaches are performing to the optimal approaches. These nearly optimal and optimal schemes are the subject of the next section.

4. Trellis-Based Receivers

The standard decoder for a convolutional code is the Viterbi algorithm operating on the encoder's trellis because it allows maximum likelihood sequence estimation with a modest decoder complexity when the constraint length of the code is small, [17]. The optimal joint decoder for an asynchronous CDMA system is also a Viterbi algorithm operating on a time-varying trellis with 2^{K-1} states, [1]. The simplest trellis-based

approach is therefore the decoder shown in Figure 9a, which will be referred to as the *partitioned* trellis-based solution. In this approach, an optimal equalizer for the MUI operates at the code symbol level and feeds the resulting hard code symbol estimates to a bank of Viterbi algorithms which operate independently of each other. These Viterbi algorithms decode the ML information sequence for each respective user given the decisions from the MUI equalizer.

The time complexity per decoded bit for this receiver may be estimated again by considering the number of metric computations per information bit decided. We again consider first the rate $1/Q$ code example. The optimal equalizer computes 2^K metrics for every bit that is decided and there are 2^W metrics computed in the decoding Viterbi algorithm for every bit decided, so the total TCB = $O(Q2^K+2^W)$. In the general rate P/Q code case, TCB = $O([Q2^K+2^{K+P}]/P)$.

Another variation of the partitioned trellis-based decoder would be to modify the equalizer Viterbi algorithm to supply soft-decision outputs to the outer decoding Viterbi algorithms. This could easily be accomplished using the techniques described in [29]. This idea is the trellis-based analog of the SCS-DFE and it is reasonable to expect that its performance would be slightly better than the standard partitioned trellis-based receiver in most cases.

One major limitation of the partitioned trellis-based decoder approach, of the soft or hard-decision variety, is that the equalization of the MUI will have to take place at the code symbol level. Because the code symbols have a smaller energy per symbol than the information symbols, it is reasonable to expect that the decoder which takes the coding into account and effectively operates at the information symbol level can attain a higher performance level. This idea is the trellis-based analog of the integrated DFE. Figure 9b illustrates the optimal maximum likelihood sequence estimator, and in sections 4.1 and 4.2, this decoder will be derived.

4.1 Optimum Sequence Estimator For Rate-1/2 Convolutional Codes

In this section, the optimal MLSE will be derived for the special case in which each user in the network is employing a rate-1/2 convolutional code with a constraint length of W. Our limitation to this special case will facilitate the derivation of the decoder considerably, and it will be outlined in section 4.2 how the optimal decoder can be derived in a similar fashion for a general rate-P/Q convolutional code case.

To begin, it is important to note that the optimal sequence estimator or equalizer for multiple-user uncoded signals operates in a round-robin fashion among all K users in the system, [1]. This Viterbi algorithm traverses one trellis stage per channel bit observed.

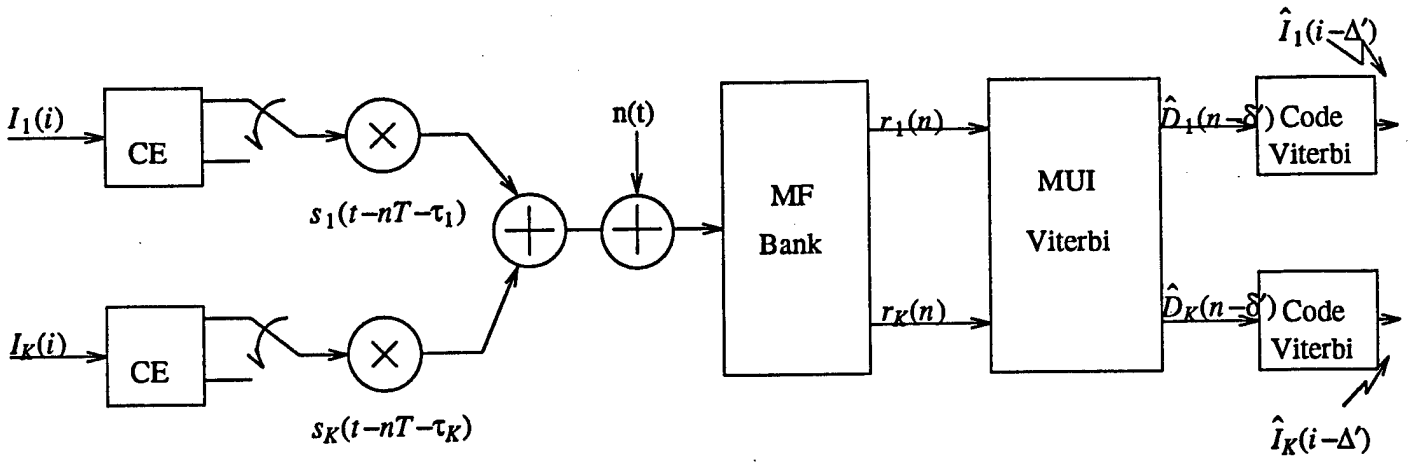

Figure 9a Partitioned Trellis-Based Equalizer/Decoder.

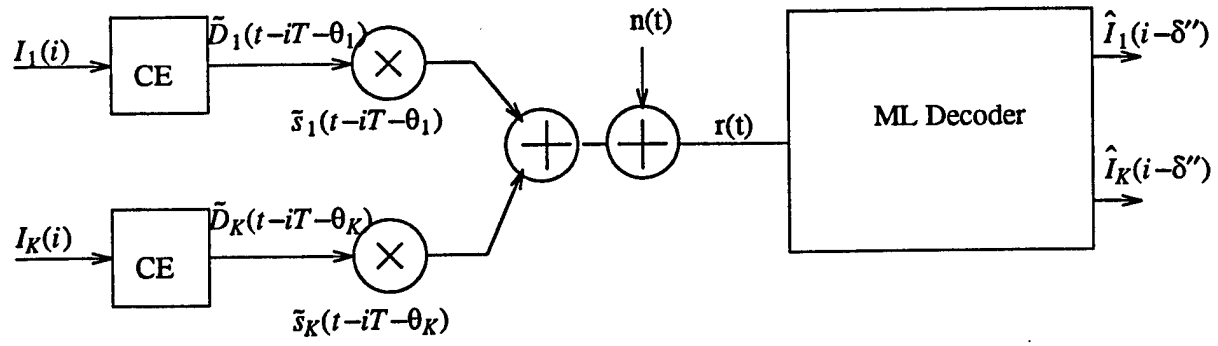

Figure 9b Maximum Likelihood Sequence Estimator for the equivalent problem.

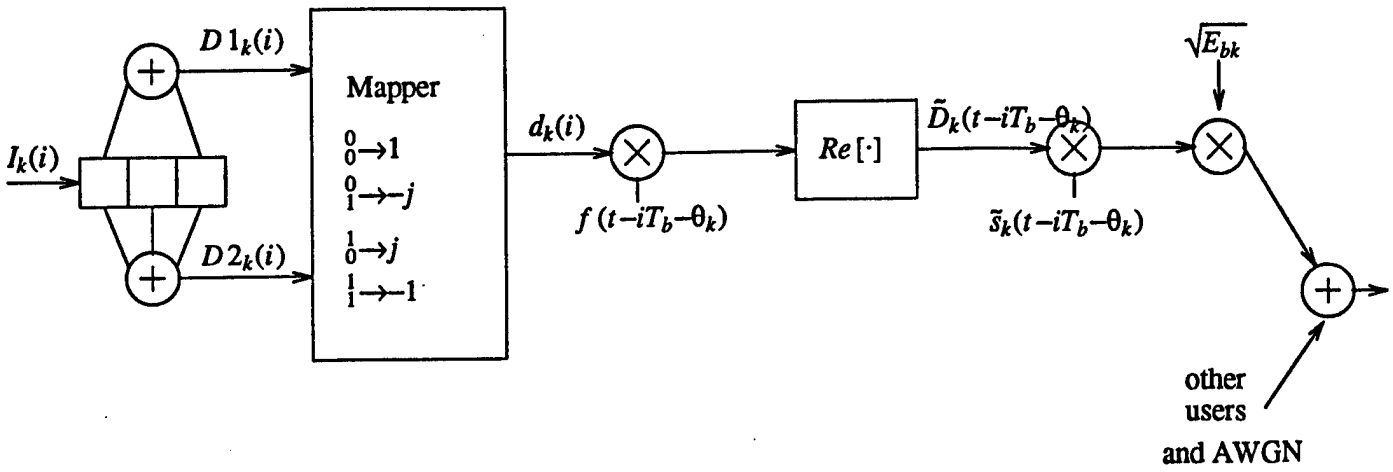

Figure 10 Trellis code view of a rate-1/2 convolutional encoder with BPSK modulation for user k at time i.

The optimal sequence estimator for decoding the rate-1/2 code for one of the users in a single user environment, however, is a Viterbi algorithm which requires two channel observations from the user of interest to move ahead one stage in the trellis. The fact that the equalizer and decoder operate in a fundamentally different way suggests that a slightly different view of the problem is required. The following view of the problem will be adopted in order to bypass this issue. The rate-1/2 convolutional code can be viewed not as a code which produces two binary bits per information bit period, T_b, but as an equivalent trellis code which produces one 4-ary coded waveform every T_b. We will reorient ourselves with respect to these super-symbols which occupy an information bit period, and then examine the effect of MUI on these super-symbols. By then formulating the equalization problem at the receiver with respect to the super-symbol view of the received signal, we can accomplish both the tasks of equalization and decoding in the same Viterbi algorithm. Because there is only one super-symbol received for each information bit that must be decided, the decoder can be formulated in the same fashion as was used in [1] for the MUI problem and [19] for the ISI problem.

We begin by defining the following functions.

$$f_0(t) = \begin{cases} 1 & t \in [0,2T) \\ 0 & otherwise \end{cases} \tag{6}$$

$$f_1(t) = \begin{cases} 1 & t \in [0,T) \\ -1 & t \in [T,2T) \\ 0 & otherwise \end{cases} \tag{7}$$

and

$$f(t) = f_0(t) + j f_1(t) \ . \tag{8}$$

If the outputs of the first and second modulo-2 adders in the convolutional encoder are given respectively by $D1_k(i)$ and $D2_k(i)$ for the i^{th} information symbol interval and the k^{th} user (see Figure 10), then the output of the equivalent trellis code can be defined with the following mapping rule.

$$d_k(i) = \begin{cases} 1 & \text{if } D1_k(i)=0 \text{ and } D2_k(i)=0 \\ -1 & \text{if } D1_k(i)=1 \text{ and } D2_k(i)=1 \\ -j & \text{if } D1_k(i)=0 \text{ and } D2_k(i)=1 \\ j & \text{if } D1_k(i)=1 \text{ and } D2_k(i)=0 \end{cases} \tag{9}$$

Now, the following function may be defined

$$\tilde{D}_k(t-iT_b-\theta_k) = Re\,[d_k(i)\, f\,(t-iT_b-\theta_k)] \tag{10}$$

where $\theta_k \equiv \tau_k$ if the code is synchronized such that $D1_k(i)$ is sent in the time interval

$t\varepsilon[iT_b+\tau_k,(i+\frac{1}{2})T_b+\tau_k)$. On the other hand, if the code is synchronized such that $D\,1_k(i)$ is sent in the time interval $t\varepsilon[(i+\frac{1}{2})T_b+\tau_k,(i+1)T_b+\tau_k)$ then $\theta_k \equiv \tau_k+T$. This parameter θ_k represents the time shift of the k^{th} user's super-code symbols relative to the same reference time that was used to define the set $\{\tau_k\}_{k=1}^{K}$. It is also worth noting that with the definition of $\{\theta_k\}_{k=1}^{K}$, the users are no longer ordered such that their delay increases with k as we assumed when we were working at the code bit level. It is convenient to assume at this point that the users are reindexed so that they once again have an increasing delay with k.

Equation (10) may be rewritten as

$$\tilde{D}_k(t-iT_b-\theta_k) = Re\,[d_k(i)]\,f_0(t-iT_b-\theta_k) - Im\,[d_k(i)]\,f_1(t-iT_b-\theta_k) \tag{11}$$

by substituting equation (8) into (10). Note that $\tilde{D}_k(t)\varepsilon\{\pm f_0(t), \pm f_1(t)\}$. This waveform has a duration of $T_b = 2T$. Next, two of the signature-carrier waveforms are scaled and concatenated to form a super-signature waveform.

$$\tilde{s}_k(t-iT_b-\theta_k) = \sqrt{1/2}\,[s_k(t-iT_b-\theta_k) + s_k(t-(i+\tfrac{1}{2})T_b-\theta_k)] \tag{12}$$

(Recall that $s_k(t)$ had support on $[0,T)$.) The received waveform may now be written in terms of these waveforms of duration T_b:

$$r(t) = \sum_{i=-\infty}^{\infty}\sum_{k=1}^{K}\tilde{D}_k(t-iT_b-\theta_k)\,\tilde{s}_k(t-iT_b-\theta_k)\sqrt{E_{bk}} + n(t) \tag{13}$$

where $\sqrt{E_{bk}} = \sqrt{2E_k}$. This may be explicitly written in terms of the complex super-code symbols, $d_k(i)$, by substituting (11) into (13).

$$\begin{aligned} r(t) = \sum_{i=-\infty}^{\infty}\sum_{k=1}^{K} & Re\,[d_k(i)]\,f_0(t-iT_b-\theta_k)\,\tilde{s}_k(t-iT_b-\theta_k)\sqrt{E_{bk}} \\ & - Im\,[d_k(i)]\,f_1(t-iT_b-\theta_k)\,\tilde{s}_k(t-iT_b-\theta_k)\sqrt{E_{bk}} + n(t) \end{aligned} \tag{14}$$

Figure 11 illustrates a two-state rate-1/2 convolutional code and its equivalent trellis representation. It is worth noting that the signal that results from two code symbol intervals in a rate-1/2 convolutional code is now modeled as a signal resulting from a rate-1/2 trellis code with one complex super-code symbol modulating a pair of orthonormal basis functions through the procedure defined above. The basis functions in this new view of the waveform are

$$\phi_{0k}(t) = f_0(t)\,\tilde{s}_k(t) \tag{15}$$

and

$$\phi_{1k}(t) = f_1(t)\,\tilde{s}_k(t) \tag{16}$$

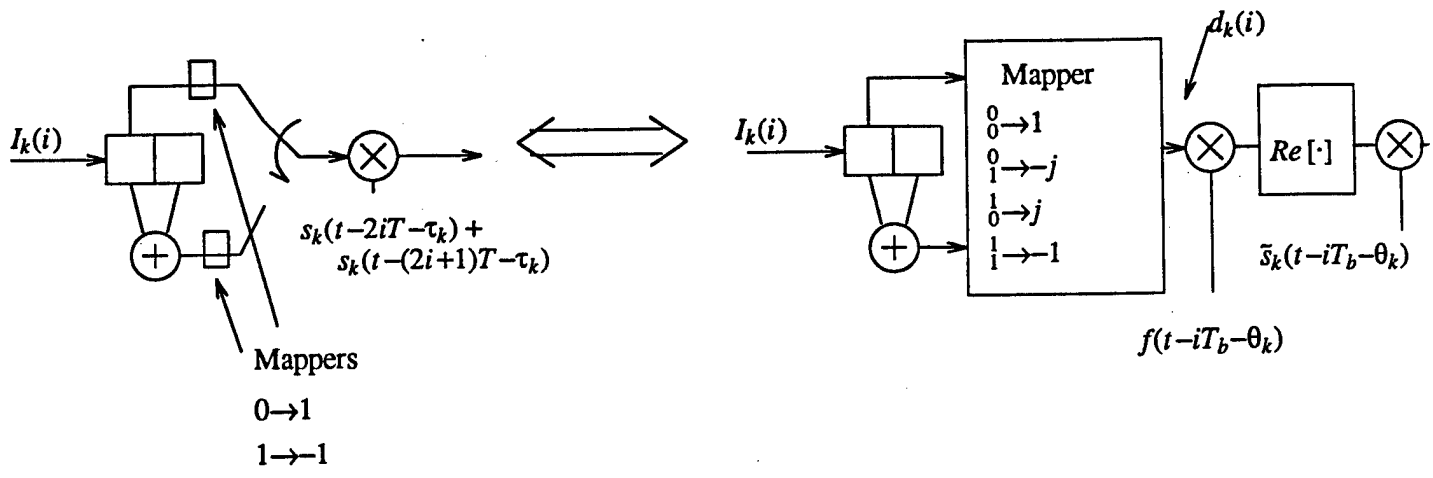

Figure 11a Rate-1/2 convolutional encoder and its equivalent trellis representation.

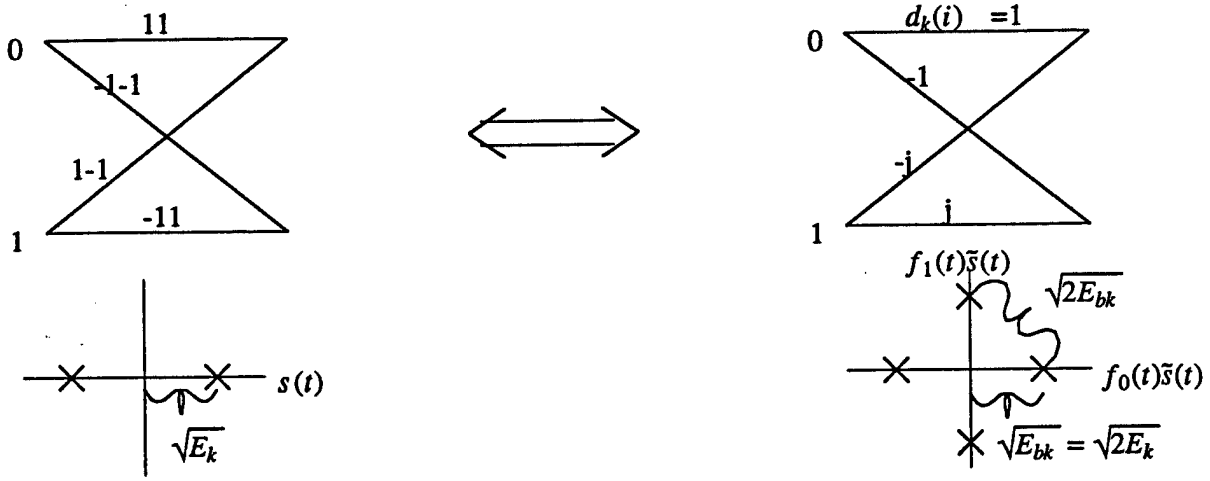

Figure 11b Trellis diagrams and signal space diagrams for each view of the code from Figure 9a.

appropriately synchronized with the information bit periods. Thus, this view of the coding process suggests that the information bits are mapped by the encoder onto waveforms in a space defined by $\phi_{0k}(t)$ and $\phi_{1k}(t)$. The resulting signal is equivalent to that emerging from the convolutional encoder and modulator, and furthermore, the performance of a Viterbi algorithm operating in the space defined by $\phi_{0k}(t)$ and $\phi_{1k}(t)$ will be identical to that of a Viterbi algorithm operating with two observations from a space defined by the basis function $s_k(t)$.

Taking the trellis viewpoint of the coder, we note that although the basis functions defined in (15) and (16) are orthonormal, they are not, in general, orthogonal to $\phi_{0j}(t)$ and $\phi_{1j}(t)$ which are the basis set for another user in the system, user j, since $s_k(t)$ and $s_j(t)$ are not orthogonal in general. The result when the received signal is a sum of K component signals is MUI.

We now define four parameters which are a measure of the degree of correlation between the basis functions of the different users.

$$\tilde{\rho}_{jk}(l) = \int_{-\infty}^{\infty} \phi_{0j}(t-\theta_j)\,\phi_{0k}(t-lT_b-\theta_k)dt \tag{17}$$

$$\tilde{U}_{jk}(l) = \int_{-\infty}^{\infty} \phi_{1j}(t-\theta_j)\,\phi_{1k}(t-lT_b-\theta_k)dt \tag{18}$$

$$\tilde{V}_{jk}(l) = \int_{-\infty}^{\infty} \phi_{0j}(t-\theta_j)\,\phi_{1k}(t-lT_b-\theta_k)dt \tag{19}$$

$$\tilde{W}_{jk}(l) = \int_{-\infty}^{\infty} \phi_{1j}(t-\theta_j)\,\phi_{0k}(t-lT_b-\theta_k)dt \tag{20}$$

These parameters play the same role in the super-symbol view of the coded signal that $\rho_{jk}(l)$ plays for the standard view of the signal. In fact, $\tilde{\rho}$, $\tilde{U}$, $\tilde{V}$ and $\tilde{W}$ can be related to ρ directly by substituting (12) into (17) through (20), as long as the relationships between θ_j and τ_j as well as θ_k and τ_k are known. If, for example, either $\theta_j = \tau_j$ and $\theta_k = \tau_k$ or $\theta_j = \tau_j + T$ and $\theta_k = \tau_k + T$ then the following holds:

$$\tilde{\rho}_{jk}(l) = \rho_{jk}(2l) + \tfrac{1}{2}\rho_{jk}(2l+1) + \tfrac{1}{2}\rho_{jk}(2l-1) \tag{21a}$$

$$\tilde{U}_{jk}(l) = \rho_{jk}(2l) - \tfrac{1}{2}\rho_{jk}(2l-1) - \tfrac{1}{2}\rho_{jk}(2l+1) \tag{21b}$$

$$\tilde{V}_{jk}(l) = \tfrac{1}{2}\rho_{jk}(2l-1) - \tfrac{1}{2}\rho_{jk}(2l+1) \tag{21c}$$

$$\tilde{W}_{jk}(l) = \tfrac{1}{2}\rho_{jk}(2l+1) - \tfrac{1}{2}\rho_{jk}(2l-1) \tag{21d}$$

Similar results hold when the relationships between the delays are different. It is also

important to note that regardless of the relationship between τ and θ, $\tilde{\rho}_{jk}(l) = \tilde{U}_{jk}(l) = \tilde{V}_{jk}(l) = \tilde{W}_{jk}(l) = 0$ for $|l|>1$; this fact will play an important role in determining the proper state description of the system for the optimal sequence estimator. Some other useful properties of the correlation parameters are $\tilde{\rho}_{jk}(l) = \tilde{\rho}_{kj}(-l)$, $\tilde{U}_{jk}(l) = \tilde{U}_{kj}(-l)$ and $\tilde{W}_{jk}(l) = \tilde{V}_{kj}(-l) = -\tilde{W}_{kj}(-l) = -\tilde{V}_{jk}(l)$.

To this point, as Figure 9b indicates, we have made no assumptions about the structure of the decoder or even the front-end processing that will supply sufficient statistics to the decoding algorithm. While a bank of matched filters matched to the signature sequences was assumed as the front end for the decision feedback techniques examined in section 3, we make no such assumption for the optimal sequence estimation receiver of this section. We will proceed with the derivation of the optimal decoder, now that the foundation has been laid and the appropriate structure of the decoding algorithm and the front end of the receiver will become apparent. This development will closely follow the derivation of the optimal MLSE in [19] and [26] for the uncoded ISI channel.

Beginning with equation (13), note that by performing a modulo-K decomposition of the index i, namely $i = \alpha(i)K + \beta(i) - 1$, we can write

$$r(t) = \sum_{i=-M}^{M} \tilde{D}_{\beta(i)}(t-\alpha(i)T_b-\theta_{\beta(i)})\,\tilde{s}_{\beta(i)}(t-\alpha(i)T_b-\theta_{\beta(i)})\sqrt{E_{b\beta(i)}} + n(t) \tag{22}$$

This assumes that the K users transmit $2M/K+1$ information bits each in the time interval of interest. In other words, instead of the initial sum of equation (13) ranging from $i=-\infty$ to ∞, it ranges from $i=-M/K$ to M/K.

Next, we use an orthonormal series representation of $r(t)$ using a basis $\{g_k(t)\}_{k=1}^{\gamma}$.

$$r(t) = \lim_{\gamma\to\infty} \sum_{k=1}^{\gamma} r^{(k)} g_k(t) \tag{23}$$

where

$$r^{(k)} = \sum_{i=-M}^{M} q_{\beta(i),k}(\alpha(i))\sqrt{E_{b\beta(i)}} + n_k \tag{24}$$

$$q_{\beta(i),k}(\alpha(i)) = \int_{-\infty}^{\infty} \tilde{D}_{\beta(i)}(t-\alpha(i)T_b-\theta_{\beta(i)})\,\tilde{s}_{\beta(i)}(t-\alpha(i)T_b-\theta_{\beta(i)})\,g_k^*(t)dt \tag{25}$$

and

$$n_k = \int_{-\infty}^{\infty} n(t) g_k^*(t)dt \tag{26}$$

which is normally-distributed with zero mean and variance of $E(n_k^* n_m) = (N_0/2)\delta(k-m)$,

where $\delta(k)$ is the Kronecker delta function.

The joint conditional probability density function for the observations given the hypothesized data sequence $\bar{D}$ is

$$P(r^{(1)},\ldots,r^{(\gamma)}\,|\,\bar{D}) = \left[\prod_{k=1}^{\gamma} 2\pi\frac{N_0}{2}\right]^{-1} \exp\left[-\sum_{k=1}^{\gamma} |\, r^{(k)} - \sum_{i=-M}^{M} q_{\beta(i),k}(\alpha(i))\sqrt{E_{b\beta(i)}}\,|^2/N_0\right] \quad (27)$$

In the limit as $\gamma\to\infty$, the logarithm of $P(r^{(1)},\ldots,r^{(\gamma)}\,|\,\bar{D})$ becomes proportional to the following waveform metric:

$$J_0(\bar{D}) = -\int_{-\infty}^{\infty} |\, r(t) - \sum_{i=-M}^{M} \tilde{D}_{\beta(i)}(t-\alpha(i)T_b-\theta_{\beta(i)})\tilde{s}_{\beta(i)}(t-\alpha(i)T_b-\theta_{\beta(i)})\sqrt{E_{b\beta(i)}}\,|^2 dt \quad (28)$$

By expanding the square we get

$$\begin{aligned} J_0(\bar{D}) = &-\int_{-\infty}^{\infty} |\, r(t)\,|^2 dt + 2\,\mathrm{Re}\Big[\sum_{i=-M}^{M}\sqrt{E_{b\beta(i)}} \\ &\cdot\Big(Re\,[d_{\beta(i)}(\alpha(i))]\int_{-\infty}^{\infty} r(t) f_0(t-\alpha(i)T_b-\theta_{\beta(i)})\tilde{s}_{\beta(i)}(t-\alpha(i)T_b-\theta_{\beta(i)})dt \\ &-Im\,[d_{\beta(i)}(\alpha(i))]\int_{-\infty}^{\infty} r(t) f_1(t-\alpha(i)T_b-\theta_{\beta(i)})\tilde{s}_{\beta(i)}(t-\alpha(i)T_b-\theta_{\beta(i)})dt\Big)\Big] \\ &-\sum_{i=-M}^{M}\sum_{m=-M}^{M}\int_{-\infty}^{\infty}\Big[Re\,[d_{\beta(i)}(\alpha(i))]f_0(t-\alpha(i)T_b-\theta_{\beta(i)}) - Im\,[d_{\beta(i)}(\alpha(i))]f_1(t-\alpha(i)T_b-\theta_{\beta(i)})\Big] \\ &\cdot\Big[Re\,[d_{\beta(m)}(\alpha(m))]f_0(t-\alpha(m)T_b-\theta_{\beta(m)}) - Im\,[d_{\beta(m)}(\alpha(m))]f_1(t-\alpha(m)T_b-\theta_{\beta(m)})\Big] \\ &\cdot\tilde{s}_{\beta(i)}(t-\alpha(i)T_b-\theta_{\beta(i)})\,\tilde{s}_{\beta(m)}(t-\alpha(m)T_b-\theta_{\beta(m)})\sqrt{E_{b\beta(i)}}\sqrt{E_{b\beta(m)}}\,dt \end{aligned} \quad (29)$$

Next, define

$$r_{0\beta(i)}(\alpha(i)) = \int_{-\infty}^{\infty} r(t) f_0(t-\alpha(i)T_b-\theta_{\beta(i)})\tilde{s}_{\beta(i)}(t-\alpha(i)T_b-\theta_{\beta(i)})dt \quad (30)$$

and

$$r_{1\beta(i)}(\alpha(i)) = \int_{-\infty}^{\infty} r(t) f_1(t-\alpha(i)T_b-\theta_{\beta(i)})\tilde{s}_{\beta(i)}(t-\alpha(i)T_b-\theta_{\beta(i)})dt \quad (31)$$

which represent the outputs of a pair of matched filters or correlators for the basis functions for user $\beta(i)$ at time $t = (\alpha(i)+1)T_b + \theta_{\beta(i)}$.

By expanding (29), and then collecting the appropriate terms we get the following metric.

$$J_0(\bar{D}_i) = J_0(\bar{D}_{i-1}) + 2\,\mathrm{Re}\Big[\, Re\,[d_{\beta(i)}(\alpha(i))]\sqrt{E_{b\beta(i)}}\;\big(r_{0\beta(i)}(\alpha(i)) -$$

$$\sum_{l=1}^{L}\Big\{Re\,[d_{\beta(i-l)}(\alpha(i-l))]\;\tilde{\rho}_{\beta(i)\beta(i-l)}(\alpha(i-l)-\alpha(i))$$

$$- Im\,[d_{\beta(i-l)}(\alpha(i-l))]\;\tilde{V}_{\beta(i)\beta(i-l)}(\alpha(i-l)-\alpha(i))\Big\}\sqrt{E_{b\beta(i-l)}}\big)$$

$$- Im\,[d_{\beta(i)}(\alpha(i))]\sqrt{E_{b\beta(i)}}\;\big(r_{1\beta(i)}(\alpha(i)) +$$

$$\sum_{l=1}^{L}\Big\{Im\,[d_{\beta(i-l)}(\alpha(i-l))]\;\tilde{U}_{\beta(i)\beta(i-l)}(\alpha(i-l)-\alpha(i))$$

$$- Re\,[d_{\beta(i-l)}(\alpha(i-l))]\;\tilde{W}_{\beta(i)\beta(i-l)}(\alpha(i-l)-\alpha(i))\Big\}\sqrt{E_{b\beta(i-l)}}\big)\Big] - 2E_{b\beta(i)} \qquad (32)$$

where $\bar{D}_i$ represents the data sequence up to time interval i, and L is the smallest integer such that for every $L' > L$ we have $\tilde{\rho}_{jk}(\alpha(L')) = \tilde{U}_{jk}(\alpha(L')) = \tilde{V}_{jk}(\alpha(L')) = \tilde{W}_{jk}(\alpha(L')) = 0$. We have already seen that the correlation parameters are zero when $|\alpha(L')| > 1$. We thus may conclude that $L = K-1$.

There are a number of important observations that can be made from the metric given in equation (32). First of all, it is additive in the sense that the global metric for evaluating the most likely sequence of super-code symbols, $\{\, d_{\beta(i)}(\alpha(i))\,\}_{i=-M}^{M}$ is written as a sum of stage metrics. Furthermore, the i^{th} stage metric depends only on the super code symbols in the set

$$\Xi = \{d_{\beta(i)}(\alpha(i)),\, d_{\beta(i-1)}(\alpha(i-1)),\ldots,\, d_{\beta(i-K+1)}(\alpha(i-K+1))\}, \qquad (33)$$

along with the matched filter outputs, $r_{0\beta(i)}(\alpha(i))$ and $r_{1\beta(i)}(\alpha(i))$, as well as the energies and correlations. As in the receivers which operated at the code symbol level, with the matched filter bank at the front end of the receiver matched to the signals $\{s_k(t-jT-\tau_k)\}$, it is again possible to estimate the crosscorrelations using the local oscillators and code generators which are assumed to be synchronized to the K components of the incoming signal. We can also estimate the energies, $\{E_{b\beta(i)}\}$ by averaging the outputs of the matched filters for a number of bits. (The number over which they would be averaged would depend on the rate at which the relative strengths of the users is varying.) It is also interesting to note that $r_{0k}(i)$ and $r_{1k}(i)$ can be constructed from the standard matched filter output that is matched to the signal $s_k(t)$ by storing successive outputs and then linearly combining them as is illustrated in Figure 12.

For any user, k, the convolutional encoder defines a mapping rule from the input information symbol and present state of the encoder to the code bits, $D1_k(j)$ and $D2_k(j)$. In addition, equation (9) defined a mapping rule from these code symbols to the complex super-code symbol, $d_k(j)$. If we define the function $h(\cdot)$ as the composite mapping rule

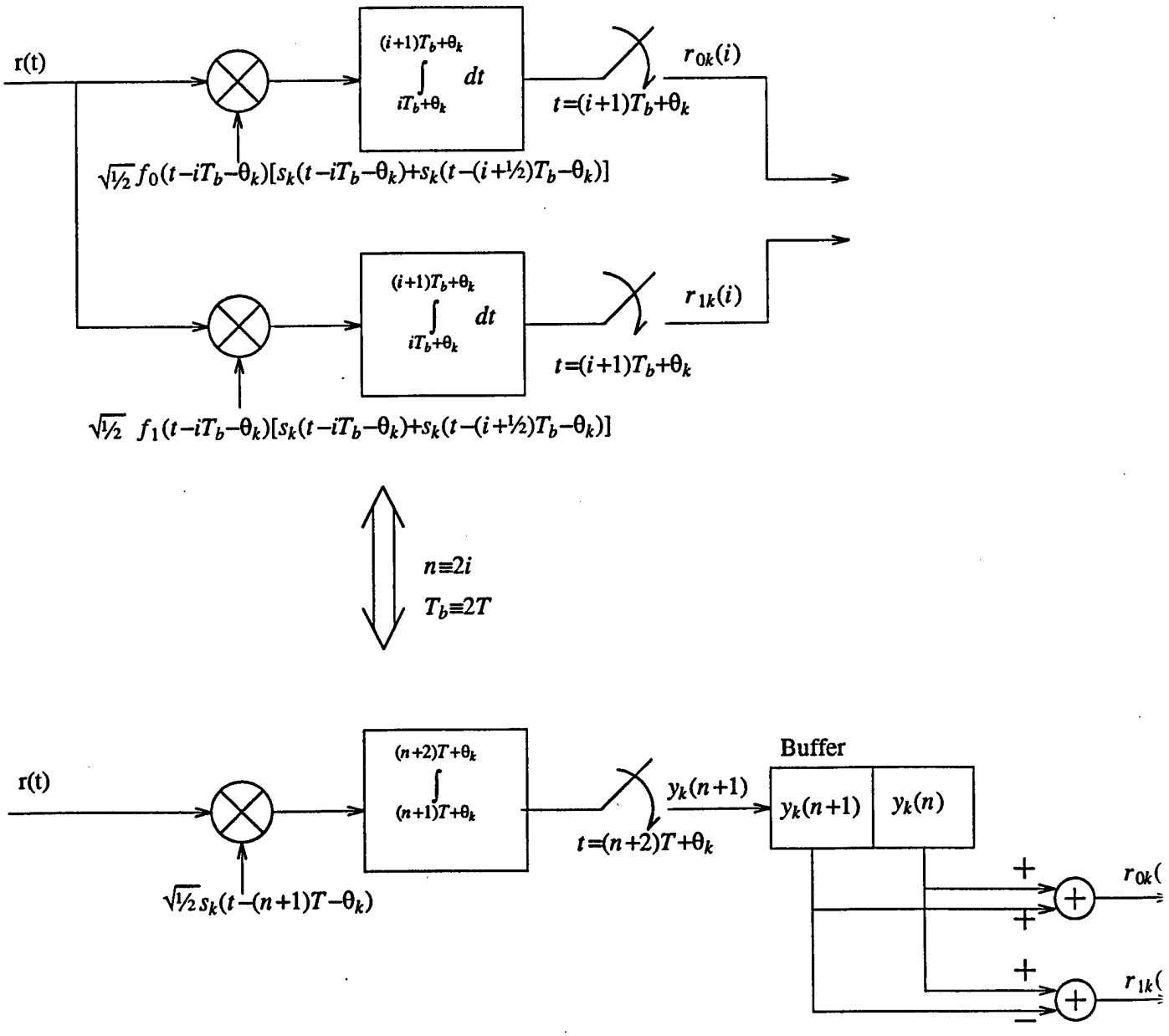

Figure 12 Correlator front end to the globally optimal MLSE and an alternate front end which constructs the same correlator outputs from the basic correlator with the standard signature/carrier waveform basis functi

from the input information symbol and state to the complex super-code symbol, then by substituting the information symbols that define the state of the encoder in for the state, the following expression may be written:

$$d_k(j) = h\left(I_k(j),\, I_k(j-1),\ldots,\, I_k(j-W+1)\right) \tag{34}$$

Thus, in this form, it is clear that the complex super-code symbol depends on only certain information symbols. Using this information, it is easy to redefine the set Ξ which was defined in equation (33) in terms of the information symbols which affect the i^{th} stage metric.

$$\tilde{\Xi} = \{I_{\beta(i)}(\alpha(i)), \sigma_i\} \tag{35}$$

$$\sigma_i = \{I_{\beta(i-1)}(\alpha(i-1)),\, I_{\beta(i-2)}(\alpha(i-2)),\ldots,\, I_{\beta(i-WK+1)}(\alpha(i-WK+1))\} \tag{36}$$

Thus it is now apparent that the system may be described in terms of 2^{WK-1} states, since the information symbols are binary. Furthermore, the maximum likelihood sequence estimator can be implemented with a Viterbi algorithm operating on a trellis with 2^{WK-1} states and two branches per state. This trellis will be cyclically time-varying as in the uncoded case. [1] Furthermore, it is clear that this trellis reduces to the trellis derived in [1] when the constraint length of the code is one. (uncoded transmission for each user)

The time complexity per bit decoded for the MLSE is $TCB = O(2^{WK})$ since there are $2 \cdot 2^{WK-1}$ metrics which must be computed at each stage of the trellis and one information bit is decided at each stage. Note that for the case of $W = 1$, the TCB calculated in [1] is again obtained.

Obviously, the number of states in the MLSE grows very quickly with both the number of users in the system and the constraint length of the codes being used. In fact, for the simple 4-user example used in the simulations of the decision feedback equalizers where each user used a $W = 3$, or 4-state code, the MLSE requires a Viterbi algorithm operating on a trellis with 2048 states!

Figure 11 provides an example of a 2-state code that may be used by each user in a CDMA system. If there are 2 users in the system using the code of Figure 11, the MLSE trellis will have 8 states and is shown in Figure 13.

4.2 MLSE For Rate-P/Q Convolutional Codes

Now that the MLSE has been derived for the rate-1/2 case, it is not difficult to generalize to the case of rate-P/Q convolutional codes. The general metric will not be derived here, but instead we will highlight the differences from the case derived above.

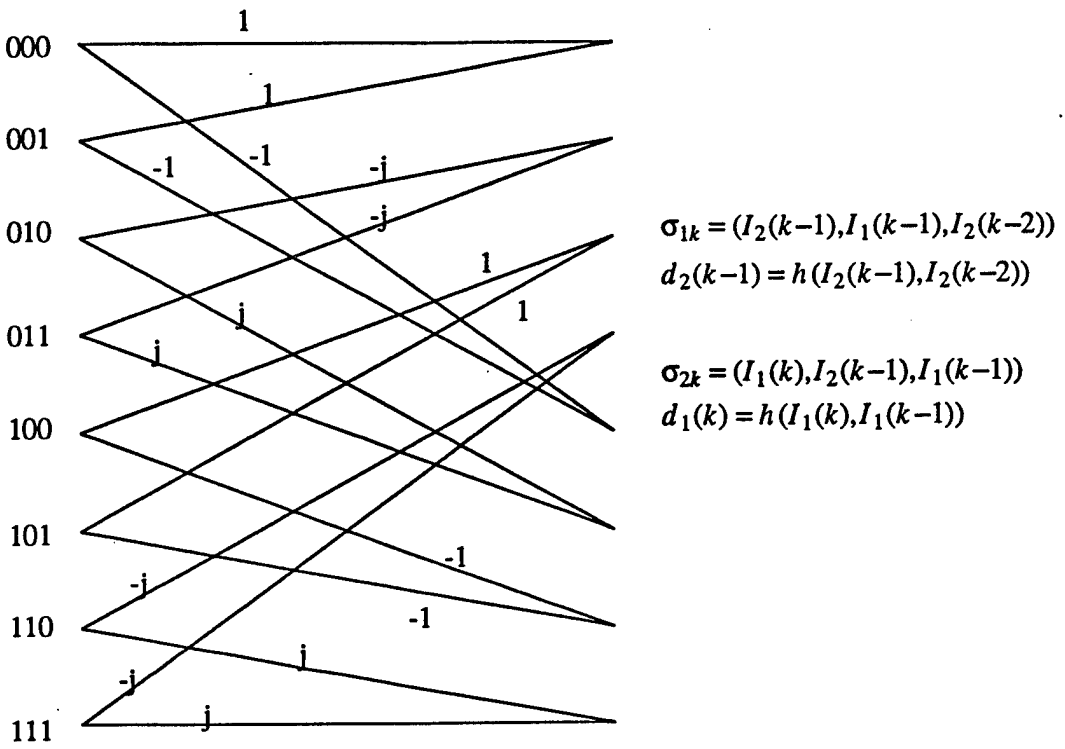

Figure 13 Trellis for the globally optimum MLSE for the 2-user, 2 state code example in Figure 11. The trellis is cyclically time-varying and the meaning of the state at some particular stage is given by either σ_{1k} or σ_{2k} for users one and two respectively in information bit period k. The complex super-code symbol $d_j(k)$ labels the trellis branches and an expression for the mapping between information symbols and super-code symbols is given.

First , consider the case of a system where each user operates with a rate-$1/Q$ convolutional code. The function $\tilde{D}_k(t)$ will again have to be constructed from a set of orthogonal basis functions. In the rate-1/2 case, this was accomplished with the basis set $\{f_o(t),f_1(t)\}$, where both basis functions span the time interval $[0,T_b)$. For the rate-$1/Q$ code case, a set could again be constructed where each basis function in the set spans the entire information bit period, however it is much simpler to use a set where each basis function is non-overlapping in time with the others and occupies an interval of length T_b/Q. It is worth noting that this same set could have been used in the rate-1/2 case to yield the same super-code function, $\tilde{D}_k(t)$. If we had used this alternate basis set for the rate-1/2 case, the resulting metric would have had a different form, but it would be equivalent to the one derived.

To illustrate a possible formulation for the rate-$1/Q$ case, let $D\,1_k(i)$ through $DQ_k(i)$ be the Q outputs of the convolutional encoder for user k at time i appropriately mapped to the antipodal set. Then the super-code function $\tilde{D}_k(t)$ could be defined as:

$$\tilde{D}_k(t-iT_b-\theta_k) = D\,1_k(i)\cdot g(t-iT_b-\theta_k) + D\,2_k(i)\cdot g(t-(i+1/Q)T_b-\theta_k) +\ldots$$
$$\ldots + DQ_k(i)\cdot g(t-(i+(Q-1)/Q)T_b-\theta_k) \qquad (37)$$

where $g(t)$ is a function with value one on the interval $nT \le t \le (n+1)T$ and zero elsewhere, and $T_b = QT$. Again, the functions $\{\tilde{s}_k(t)\}$ would be constructed from scaled concatenations of Q versions of $s_k(t)$. To derive the metric, we could begin with (28) and proceed in the same fashion as in section 4.1. The number of states in the trellis used by the Viterbi algorithm will again be 2^{WK-1}, and the $TCB = O(2^{WK})$. While the number of states in system is not affected by the rates of the codes used by each user, it is worth keeping in mind that the metrics used to evaluate paths become increasingly complex as Q increases.

For the general rate-P/Q case, we again use the definition $\kappa = \log_2 S$ where S is the number of states in the single user's encoder. Thus, κ represents the total binary memory order of each user's encoder. There are 2^P input hypotheses to test in each information bit period for each user, so the overall trellis will have 2^P branches per state. Furthermore, the state of the system will be specified by $(\kappa+P)(K-1)+\kappa$ information bits, so it will have $2^{\kappa K+PK-P}$ states. This will result in a $TCB = O(2^{\kappa K+PK}/P)$. A comparison with the TCB estimates of the DFE structures discussed in section 3 shows how vastly much more complex the MLSE is than the DFE approaches in most cases.

Clearly the exponential dependence of the TCB on the number of users, the number of states in each of the user's codes and P makes the use of the optimal decoder prohibitive for a realistic system. It is, however, an important receiver because it represents the

best that can be achieved in terms of sequence error probability, and it will provide a good baseline on which to judge the quality of suboptimal schemes. This receiver also raises the possibility of using a variety of sparse searching algorithms like a sequential decoder as was used in [24] for the uncoded case, or reduced state sequence estimation techniques like those proposed in [10] for the uncoded MUI equalization problem and [27] and [28] for the combined equalization and decoding problem for single-user links suffering from ISI.

4.3 Performance of the Optimal Sequence Estimator

To illustrate the derivation of some performance bounds for the MLSE, we will again use the rate 1/2 code example. In this analysis we will follow fairly closely the analysis which appeared in both [1] and [19]. In keeping with [1], we consider the decoding window to range from the index $-M$ to the index M, which corresponds to each of the K users transmitting for information bit periods ranging from $-M/K$ to M/K. The goal of this section is to estimate the performance of the optimal sequence estimator by bounding the finite and infinite horizon error probabilities for the k^{th} user in the system, denoted $P_k^M(i)$ and $P_k = \lim_{M\to\infty} P_k^M(i)$. To simplify the notation, we will use the following definitions:

$$E_b^i = E_{b\beta(i)} \tag{38}$$

$$d_i = d_{\beta(i)}(\alpha(i)) \tag{39}$$

$$\tilde{\rho}_{im} = \tilde{\rho}_{\beta(i)\beta(m)}(\alpha(m)-\alpha(i)) \tag{40}$$

$$\tilde{U}_{im} = \tilde{U}_{\beta(i)\beta(m)}(\alpha(m)-\alpha(i)) \tag{41}$$

$$\tilde{V}_{im} = \tilde{V}_{\beta(i)\beta(m)}(\alpha(m)-\alpha(i)) \tag{42}$$

$$\tilde{W}_{im} = \tilde{W}_{\beta(i)\beta(m)}(\alpha(m)-\alpha(i)) \tag{43}$$

$$r_{0i} = r_{0\beta(i)}(\alpha(i)) = \sum_{j=i-K+1}^{i+K-1} Re\,[d_j]\sqrt{E_b^i}\,\tilde{\rho}_{ij} - Im\,[d_j]\sqrt{E_b^i}\,\tilde{V}_{ij} + z_{oi} \tag{44}$$

$$r_{1i} = r_{1\beta(i)}(\alpha(i)) = \sum_{j=i-K+1}^{i+K-1} Re\,[d_j]\sqrt{E_b^i}\,\tilde{W}_{ij} - Im\,[d_j]\sqrt{E_b^i}\,\tilde{U}_{ij} + z_{1i} \tag{45}$$

where z_{0i} and z_{1i} are the noise statistics at the output of the matched filters for the basis functions $\phi_{0\beta(i)}$ and $\phi_{1\beta(i)}$ respectively for that user's data interval $\alpha(i)$.

We next consider the transmission of the sequence of super-code symbols, $\bar{d} = \{d_n\}_{n=-M}^{M}$, and a competing sequence $\bar{d}+\bar{e}$ corresponding to the sequence $\{d_n+e_n\}_{n=-M}^{M}$ where $\bar{e} = \{e_n\}_{n=-M}^{M}$ is a sequence of error symbols. Each e_n can take on values in the

set $F = \{0, \pm 2, \pm 2j, \pm 1 \pm j\}$. Next, define the following sets:

$$B = \{\, \bar{e}: e_k(i) \varepsilon F,\ i=-M,\ldots,M,\ k=1,\ldots,K,\ e_k(i) \neq 0 \text{ for } \textit{some } i,k \,\} \tag{46}$$

$$A(\bar{d}) = \{\, \bar{e}: \bar{e} \varepsilon B,\ \bar{d} + \bar{e} \varepsilon C \,\} \tag{47}$$

$$C = \{\, \bar{d}: \bar{d} \varepsilon h(\{\bar{I}\})\} \tag{48}$$

where $h(\cdot)$ is the mapping rule defined by the code from an information sequence, $\bar{I}$, to a sequence of super-code symbols, $\bar{d}$. Since this mapping rule is a one to one function, it has an inverse. If we define the information error sequence

$$\bar{\psi} = h^{-1}(\bar{d} + \bar{e}) - \bar{I} \tag{49}$$

which is the information bit error sequence corresponding to $\bar{d} + \bar{e}$ such that if $\bar{d} = h(\bar{I})$, then $\bar{d} + \bar{e} = h(\bar{I} + \bar{\psi})$. This allows us to define

$$A_k^M(\bar{d}, i) = \{\bar{e}: \bar{e} \varepsilon A(\bar{d}),\ \psi_k(i) \neq 0\} \tag{50}$$

so $A_k^M(\bar{d}, i)$ is the set of admissible error sequences which affect the i^{th} information bit of the k^{th} user. From these definitions, it follows that the conditional probability of error for the i^{th} bit of the k^{th} user given the transmitted super code symbol sequence $\bar{d}$ is given by

$$P_k^M(i \mid \bar{d}\ sent) = P\left[\bigcup_{\bar{e} \varepsilon A_k^M(\bar{d}, i)} \{J_0(\bar{d} + \bar{e}) > J_0(\bar{d}) \mid \bar{d}\ sent\} \right] \tag{51}$$

and so the probability of error for the i^{th} information bit of the k^{th} user may be written as

$$P_k^M(i) = \sum_{\bar{d} \varepsilon C} P_k^M(i \mid \bar{d}\ sent) \cdot P^M(\bar{d}\ sent) \tag{52}$$

Since an expression for $P_k^M(i \mid \bar{d}\ sent)$ is not known, we choose to bound it with a union bound.

$$P_k^M(i) \leq \sum_{\bar{d} \varepsilon C} \sum_{\bar{e} \varepsilon A_k^M(\bar{d}, i)} P(J_0(\bar{d} + \bar{e}) > J_0(\bar{d}) \mid \bar{d}\ sent) \cdot P^M(\bar{d}\ sent) \tag{53}$$

It can be shown that by modifying the expression given in equation (28) and substituting the above definitions we obtain the following form of the metric

$$J_0(\bar{d}) = 2\mathrm{Re}\left[\sum_{i=-M}^{M} \sqrt{E_b^i} (Re\,[d_i] r_{0i} - Im\,[d_i] r_{1i}) \right] - \sum_{i=-M}^{M} \sum_{m=-M}^{M} (Re\,[d_i]\mathrm{Re}[d_m] \tilde{\rho}_{im}$$

$$+ Im\,[d_i]\mathrm{Im}[d_m] \tilde{U}_{im} - Re\,[d_i]\mathrm{Im}[d_m] \tilde{V}_{im} - \mathrm{Im}[d_i] Re\,[d_m] \tilde{W}_{im}) \sqrt{E_b^i E_b^m} \tag{54}$$

The event $J_0(\bar{d} + \bar{e}) > J_0(\bar{d})$ may now be expanded using equation (54) and substituting (44) and (45) for r_{0i} and r_{1i} respectively. After some algebra, the following

expression for this event is obtained.

$$\sum_{i=-M}^{M}\sum_{m=-M}^{M}(Re\,[e_i]\mathrm{Re}[e_m]\tilde{\rho}_{im}+Im\,[e_i]\mathrm{Im}[e_m]\tilde{U}_{im}$$

$$-Re\,[e_i]\mathrm{Im}[e_m]\tilde{V}_{im}-\mathrm{Im}[e_i]Re\,[e_m]\tilde{W}_{im})\sqrt{E_b^i E_b^m}$$

$$<\sum_{i=-M}^{M}2\sqrt{E_b^i}\,(Re\,[e_i]z_{0i}-Im\,[e_i]z_{1i}) \tag{55}$$

Let the left side of the inequality in (55) be denoted by $\Delta^2(\bar{e})$. The right side of equation (55) is a linear combination of Gaussian random variables, z_{0i} and z_{1i}. We know that

$$E[z_{0i}]=E[z_{1i}]=0 \tag{56}$$

and also that

$$E[z_{0i}\,z_{0m}]=\frac{N_0}{2}\tilde{\rho}_{im} \tag{57}$$

$$E[z_{1i}\,z_{1m}]=\frac{N_0}{2}\tilde{U}_{im} \tag{58}$$

$$E[z_{0i}\,z_{1m}]=\frac{N_0}{2}\tilde{V}_{im} \tag{59}$$

$$E[z_{1i}\,z_{0m}]=\frac{N_0}{2}\tilde{W}_{im} \tag{60}$$

As a result, if we define γ to be the right side of equation (55), namely

$$\gamma=\sum_{i=-M}^{M}2\sqrt{E_b^i}\,(Re\,[e_i]z_{0i}-Im\,[e_i]z_{1i}) \tag{61}$$

then it is not difficult to show that $E[\gamma]=0$ and $Var[\gamma]=2N_0\,\Delta^2(\bar{e})$. Next, the two-sequence error probability, or the probability of the event given in equation (55), becomes the probability that the Gaussian random variable, γ, is larger than the threshold, $\Delta^2(\bar{e})$. Thus

$$P\,(J_0(\bar{d}+\bar{e})>J_0(\bar{d})\mid \bar{d}\ sent)=Q\left[\frac{\Delta^2(\bar{e})}{\sqrt{2N_0\Delta^2(\bar{e})}}\right] \tag{62}$$

We next define the following efficiency parameter for the pair of sequences separated by the code symbol error sequence, $\bar{e}$, as

$$\eta_k^M(\bar{e})=\frac{\Delta^2(\bar{e})}{4E_{bk}}\,. \tag{63}$$

This allows us to rewrite (62) as

$$P(J_0(\bar{d}+\bar{e}) > J_0(\bar{d}) \mid \bar{d}\ sent) = Q\left[\sqrt{\frac{2E_{bk}}{N_0}\cdot\eta_k^M(\bar{e})}\right] \tag{64}$$

so $\eta_k^M(\bar{e})$ may be viewed as an asymptotic efficiency relative to uncoded BPSK transmission for the k^{th} user for the pair of sequences $\bar{d}$ and $\bar{d}+\bar{e}$. It is also worth noticing that the signal generated by modulating the error sequence

$$S(\bar{e},t) = \sum_{i=-M/K}^{M/K}\sum_{n=1}^{K} Re\,[e_n(i)]\phi_{1n}(t-iT_b-\theta_n)\sqrt{E_{bn}} - Im\,[e_n(i)]\phi_{2n}(t-iT_b-\theta_n)\sqrt{E_{bn}} \tag{65}$$

has energy

$$||S(\bar{e},t)||^2 = \int_{-\infty}^{\infty} |S(\bar{e},t)|^2 dt = \Delta^2(\bar{e}) \tag{66}$$

This implies that an alternate way to express the efficiency parameter defined in (63) for the pair of sequences $\bar{d}$ and $\bar{d}+\bar{e}$ is

$$\eta_k^M(\bar{e}) = \frac{||S(\bar{e},t)||^2}{4E_{bk}} \tag{67}$$

which is analogous to the form of the distance measure in [1] for the uncoded system.

In order to construct a lower bound on the probability of error for user k, we define the following minimum efficiency as

$$\eta_{k,min}^M(i) = \inf_{\bar{d}\in C}\ \inf_{\bar{e}\in A_k^M(d,i)}\ \eta_k^M(\bar{e}) \tag{68}$$

and so

$$P_k^M(i) \geq P\,[\eta_k^M(\bar{d},i) = \eta_{k,min}^M(i)]\cdot Q\left[\sqrt{\frac{2E_{bk}}{N_0}\cdot\eta_{k,min}^M(i)}\right] \tag{69}$$

So we now have a lower bound expression for $P_k^M(i)$ given in (69) and an upper bound expression when (64) is substituted into equation (53).

To obtain bounds for the infinite horizon error probability, $P_k = \lim_{M\to\infty} P_k^M(i)$, we may use the same argument used in [1], as it applies equally well to the coded case, namely for any error sequence $\bar{e}$ such that $e_j = e_n \neq 0$ for $j \neq n$, the sequence

$$\bar{e}' = \begin{cases} e_m & m \leq j \\ e_{m+n-j} & m > j \end{cases} \tag{70}$$

satisfies $\Delta^2(\bar{e}') \leq \Delta^2(\bar{e})$ or equivalently $\eta_k^M(\bar{e}') \leq \eta_k^M(\bar{e})$ or else it would be possible to construct a sequence with a negative energy. Thus we may conclude exactly as in [1] that the infinite horizon efficiencies $\eta_k(\bar{d})$ and $\eta_{k,min}$ are achieved by finite length error sequences. As a result, the infinite horizon error probability for the k^{th} user may be lower bounded by

$$P_k \geq P[\eta_k(\bar{d}) = \eta_{k,min}] \cdot Q\left[\sqrt{\frac{2E_{bk}}{N_0} \cdot \eta_{k,min}}\right] \tag{71}$$

Similarly, by passing (53) to the limit as M approaches infinity

$$P_k \leq \sum_{\bar{d} \in C} \sum_{\bar{e} \in A_k(\bar{d},i)} P(\bar{d}\ sent) \cdot Q\left[\sqrt{\frac{2E_{bk}}{N_0} \cdot \eta_k(\bar{e})}\right] \tag{72}$$

Where $A_k(\bar{d},i) = \lim_{M \to \infty} A_k^M(\bar{d},i)$.

In the high signal to noise ratio regime, the terms in (72) with the minimum efficiency will dominate the asymptotic behavior of the receiver. As a result, we will refer to the minimum efficiency, $\eta_{k,min}$ as the *asymptotic multiuser coding gain* for user k. The asymptotic multiuser coding gain is an efficiency parameter which is a measure of the energy gain or loss of the system relative to an uncoded BPSK system operating alone with an energy per information bit of E_{bk}. The asymptotic gain relative to this reference BPSK system in decibels is $10\log_{10}\eta_{k,min}$.

In the limiting case where there is only $K=1$ user in the system, $\eta_{k,min}$ is the asymptotic coding gain of that user's code. If there are K users in the system with orthogonal super-signature sequences, then $\eta_{k,min}$ is again the coding gain of a single user system operating with the same code. In the limiting case where the users do not employ coding, $\eta_{k,min}$ is equivalent to the asymptotic multiuser efficiency obtained in [1] for the optimal multiuser receiver for the uncoded system. Thus the asymptotic multiuser coding gain unifies the asymptotic coding gain and the asymptotic multiuser efficiency parameters. This parameter will also allow the study of near-far resistance for this receiver, which is the infimum of $\eta_{k,min}$ over the energies of all of the interfering users.

In general, the computation of $\eta_{k,min}$ is a difficult problem. In a subsequent report, we will examine the problem of the computation of $\eta_{k,min}$ for some specific cases and will provide some conditions for this parameter to be no smaller than the free distance of the code for user k. In this report, to provide some direct comparisons between the performance of the MLSE and a representative of the DFE receiver class, we will use a computer simulation for some two-user cases.

Figures 14 through 16 show the results of a simulation of a two-user system where each user employs the 4-state convolutional code shown in Figure 10. The resulting super-trellis used by the MLSE has 32 states. The MLSE, integrated DFE and conventional decoder (or one-stage integrated DFE) were simulated for the various conditions of each figure. In each figure, the cross-correlation between the code symbol level signatures, $\rho_{jk}(l)$ is defined for each j, k and l. It is then assumed for convenience that the information bit periods have delays such that $\theta_k = \tau_k$ for each user, k. This assumption implies that the relationships defined in (21) describe the correlation parameters for the MLSE.

In Figure 14, the case where $\rho_{12}(0) = 0.3$ and $\rho_{12}(-1) = 0.3$ is simulated. For this degree of MUI, the MLSE is able to perform at the single-user performance level over the range of E_b/N_0 simulated, while the 2 and 3 stage integrated DFEs suffer some loss. In this case, the conventional receiver suffers about 1.5 dB at $P_{b\ average} = 10^{-2}$.

Figure 15 illustrates a more severe MUI environment where $\rho_{12}(0) = 0.4$ and $\rho_{12}(-1) = 0.4$. In this case, the MLSE is again nearly able to recoup all of the loss that the conventional decoder suffers when compared with the performance in the single-user environment. At $P_b \approx 3 \cdot 10^{-3}$ the integrated DFE approaches lose about 1.5 dB.

In Figure 16, the same 0.4 channel is simulated for a varying near-far energy ratio. This figure shows that both the MLSE and the integrated DFE approaches appear to be near-far resistant, although this has yet to be shown analytically. Again the MLSE is not outperformed by any of the other structures at any operating point.

It is worth noting that all of the work in this section has been based upon the metric for the case where each user in the system employs rate-1/2 convolutional codes. The expression for the distance and asymptotic multiuser coding gain will be more complicated in the general rate-P/Q code case, but the derivation procedure will be the same. Thus the work in this section is meant to illustrate the general procedure for the error analysis of the more complex general code rate case.

To summarize the results of this section, we have derived the distance measure between sequences in the super-trellis of a rate-1/2 coded CDMA system. We then wrote this distance in the form of the asymptotic multiuser coding gain, $\eta_{k,min}$. This parameter unifies the asymptotic coding gain and the asymptotic multiuser efficiency parameters. Finally, a simulation illustrated the behavior of the MLSE in a variety of situations for a 2-user example.

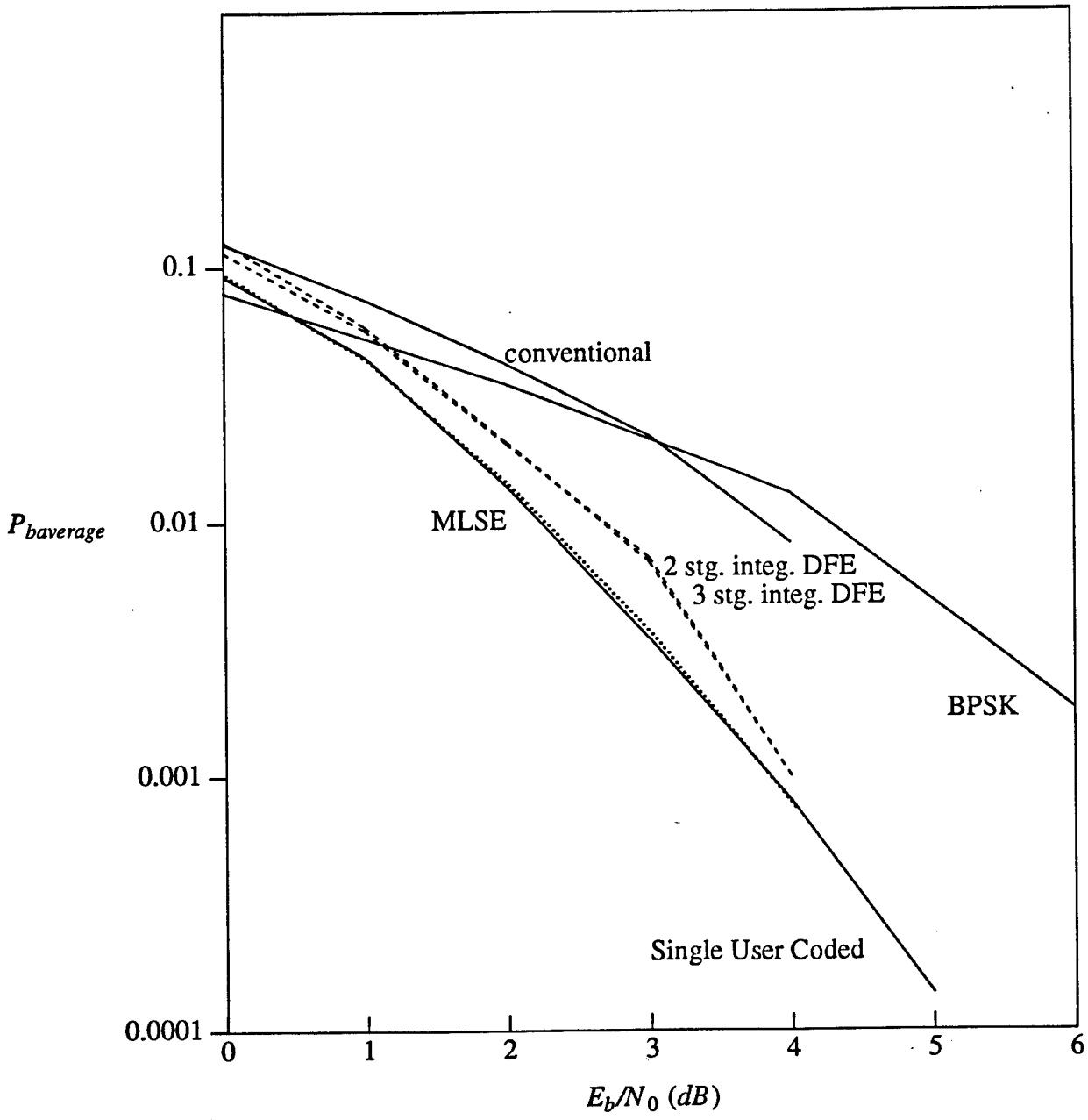

Figure 14 Performance curves of the MLSE and integrated decision feedback receivers for a 2-user channel with $\rho_{12}(0) = 0.3$ and $\rho_{12}(-1) = 0.3$ and equal energies. The solid lines show a single user system (no MUI) with and without the rate-1/2 4-state convolutional code. The two and three stage integrated DFEs are shown as dashed lines and the MLSE is shown as a dotted line.

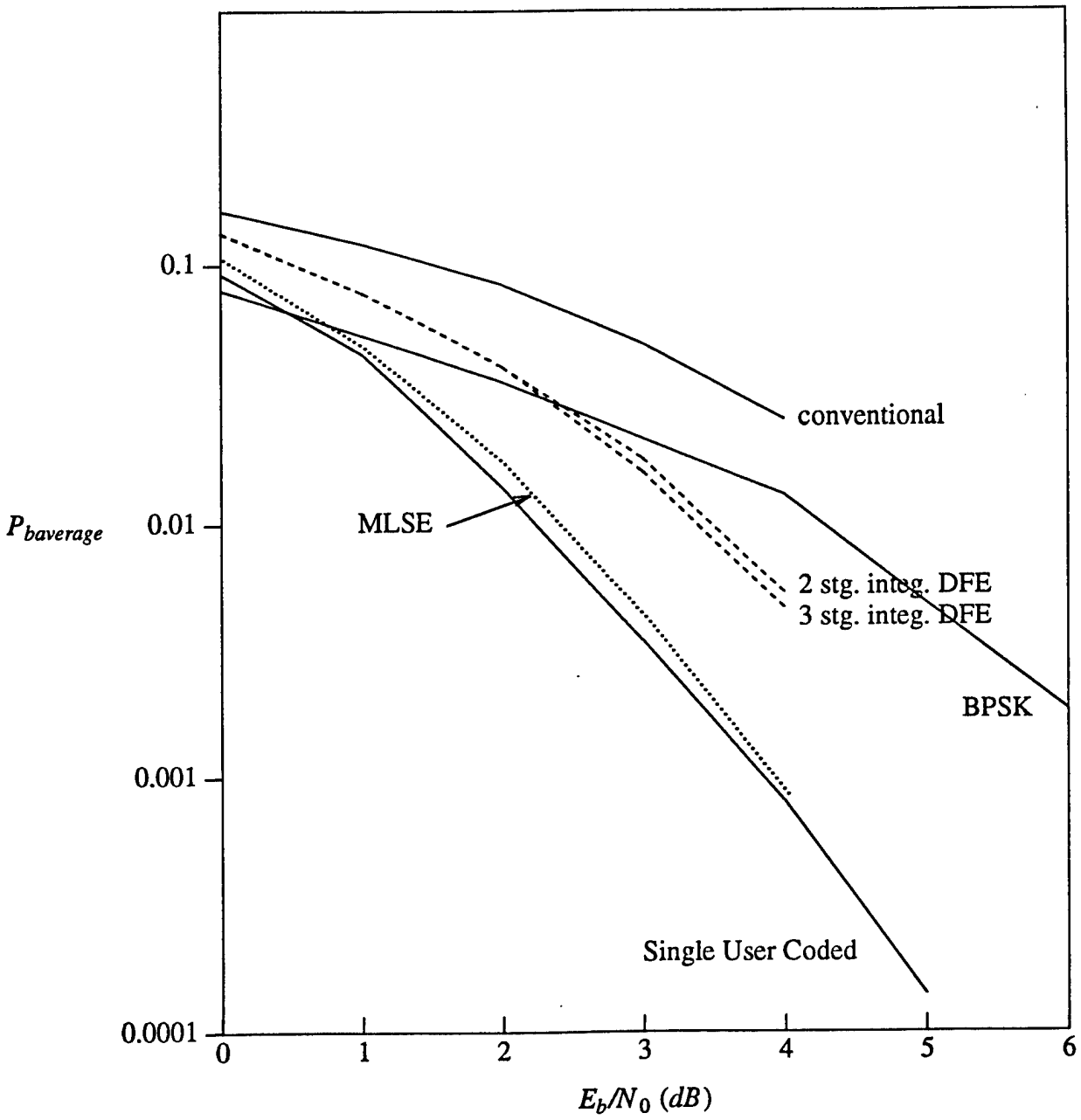

Figure 15 Performance curves of the MLSE and integrated decision feedback receivers for a 2-user channel with $\rho_{12}(0) = 0.4$ and $\rho_{12}(-1) = 0.4$ and equal energies. The solid lines show a single user system (no MUI) with and without the rate-1/2 4-state convolutional code. The two and three stage integrated DFEs are shown as dashed lines and the MLSE is shown as a dotted line.

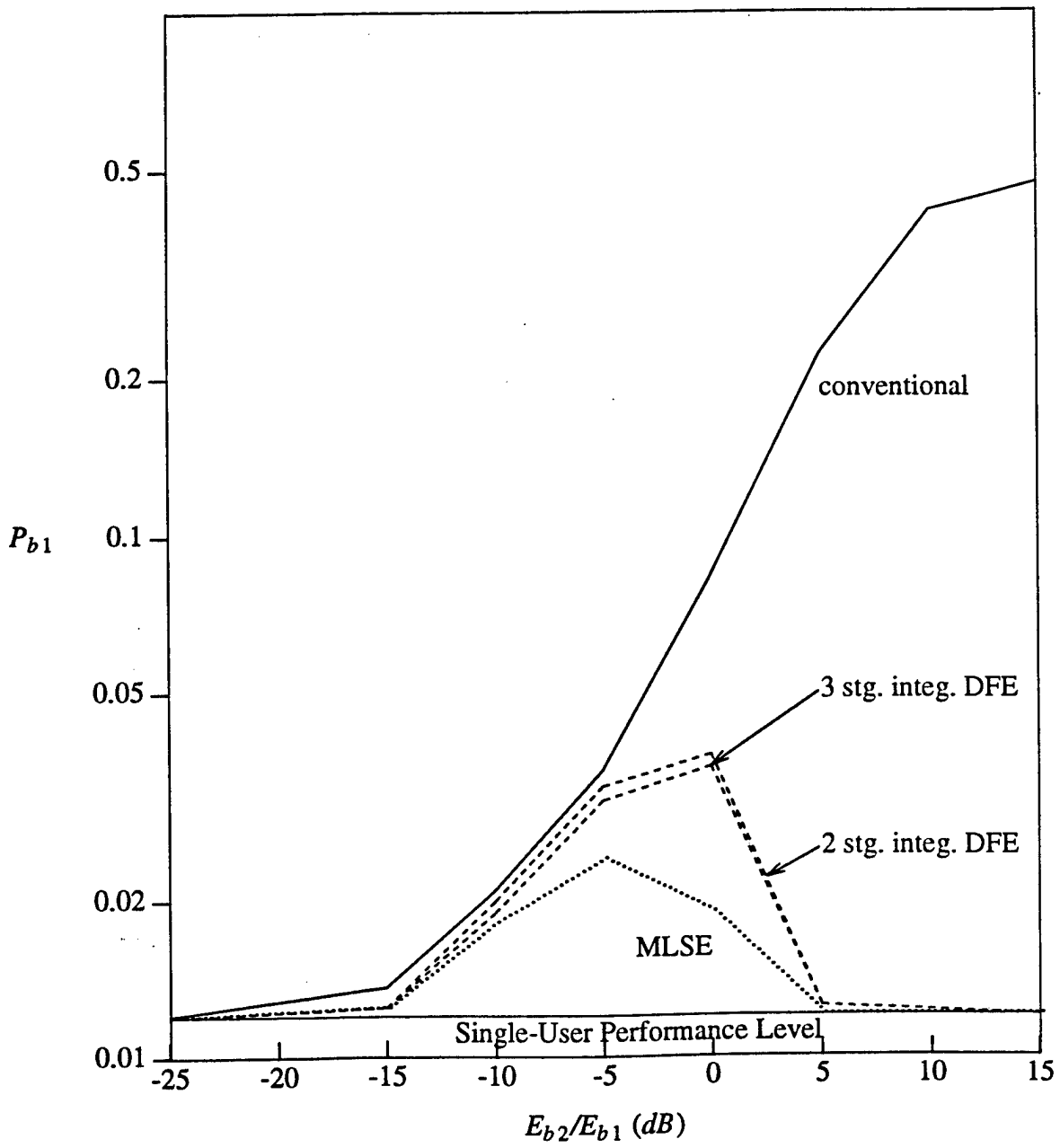

Figure 16 Near-far ratio performance curves of the MLSE and integrated decision feedback receivers for a 2-user channel with $\rho_{12}(0) = 0.4$ and $\rho_{12}(-1) = 0.4$ at $E_{b1}/N_0 = 2$ *dB*. The single-user system performance level (no MUI) with the rate-1/2 4-state convolutional code is shown as a solid line and the MLSE performance is shown as a dotted line. The two and three stage integrated DFEs are shown as dashed lines and the conventional is shown as a solid line.

5. Conclusions

In this report, both decision feedback and trellis-based multiuser decoders were studied for links which use CDMA and convolutional codes. A variety of decision feedback approaches were studied and some simulation results were presented. These results show that the DFE techniques were able to significantly improve the performance of the conventional basestation architecture. In most cases, the performance of the integrated DFE was superior to that of the SCS-DFE approaches which considered the equalization and decoding operations separately. The drawbacks of the integrated DFE architecture are its increased complexity and decoding delay over that of the SCS-DFE approaches.

In the second half of this report, two trellis-based receivers were examined. The first was a structure which attacked the MUI and the decoding operations separately. The second approach was an optimum sequence estimator for the problem. It was shown that the complexity of the MLSE depends exponentially on the number of users in the system, the number of states in each user's encoder and the number of input information bits, P. This high complexity points to the use of suboptimal trellis based approaches such as reduced state sequence estimation, [10] and [27], and sequential decoding approaches such as in [24] to provide a complexity versus performance tradeoff.

Next, an outline of the performance analysis of the system was given. In this analysis, we presented the asymptotic multiuser coding gain parameter which unifies the asymptotic coding gain parameter of coded systems with the asymptotic efficiency parameter of uncoded multiuser systems. Finally, to provide a direct comparison of the performance of the MLSE to the DFE approaches, a simulation of the MLSE and the integrated DFE was performed.

6. References

[1] S. Verdu, "Minimum Probability of Error for Asynchronous Gaussian Multiple Access Channels," *IEEE Trans. Inform. Theory*, vol. IT-32, pp 85-96, Jan. 1986.

[2] M. Varanasi and B. Aazhang, "Multistage Detection in Asynchronous CDMA Communications," *IEEE Trans. on Comm.*, vol.38, no.4, pp 509-519, April 1990.

[3] Z. Xie, R.T. Short and C.K. Rushforth, "A Family of Suboptimum Detectors for Coherent Multiuser Communications," *IEEE Journ. on Select. Areas in Comm.*, vol.8, no.4, May 1990, pp 683-690.

[4] R. Lupas and S. Verdu, "Near-Far Resistance of Multiuser Detectors in Asynchronous Channels," *IEEE Trans. on Comm.*, vol.38, no.4, April 1990, pp 496-508.

[5] A. Kajiwara and M. Nakagawa, "Crosscorrelation Cancellation in SS/DS Block Demodulator," *IEICE Trans.*, vol. E 74, no.9, pp 2596-2601, Sept. 1991.

[6] R. Kohno, H. Imai, M. Hatori, and S. Pasupathy, "An Adaptive Canceller of Cochannel Interference for Direct-Sequence Spread-Spectrum Multiple-Access Communication Networks in a Power Line," *IEEE Journ. on Select. Areas in Comm.*, vol.8, no.4, May 1990, pp 691-699.

[7] Kohno et. al., "Combination of an Adaptive Array Antenna and a Canceller of Interference for Direct-Sequence Spread-Spectrum Multiple-Access Systems," *IEEE Journ. on Select. Areas in Comm.*, vol.8, no.4, May 1990, pp 675-681.

[8] B. Aazhang, B.P. Paris, and G.C. Orsak, "Neural Networks for Multiuser Detection in Code-Division Multiple-Access Communications," *IEEE Trans. on Comm.*, vol.40, no.7, July 1992, pp 1212-1222.

[9] A. Duel-Hallen, "Equalizers for Multiple Input/Multiple Output Channels and PAM Systems with Cyclostationary Input Sequences," *IEEE Journ. on Select. Areas in Comm.*, vol.10, no.3, April 1992, pp 630-639.

[10] M.K. Varanasi "Reduced State Sequence Detection for Asynchronous Gaussian Multiple-Access Channels", *Proceedings of ISIT*, San Antonio, Texas, January, 1993, pp. 42.

[11] T. Giallorenzi, S. Wilson, "Decision Feedback Techniques for CDMA System Equalization," submitted to *IEEE Trans. on Comm.*.

[12] S. Verdu, "Optimum Multiuser Asymptotic Efficiency," *IEEE Trans. on Comm.*, vol.34, no.9, May 1991, pp. 890-897.

[13] H.V. Poor, S. Verdu, "Single-User Detectors for Multiuser Channels," *IEEE Trans. on Comm.*, vol. 36, no. 1, Jan. 1988, pp.50-60.

[14] K.S. Schneider, "Optimum Detection of Code Division Multiplexed Signals," *IEEE Trans. on Aerospace* and *Electronic Systems*, vol.AES-15, no. 1, Jan. 1979, pp. 181-185.

[15] W.V. Etten, "Maximum Likelihood Receiver for Multiple Channel Transmission Systems," *IEEE Trans. on Comm.*, Feb. 1976, pp. 276-283.

[16] G.D. Boudreau, D.D. Falconer, S.A. Mahmoud, "A Comparison of Trellis Coded Versus Convolutionally Coded Spread-Spectrum Multiple-Access Systems," *IEEE Journ. on Select. Areas in Comm.*, vol.8, no.4, May 1990, pp 628-640.

[17] G.D. Forney, "The Viterbi Algorithm," *Proceedings of the IEEE*, vol. 61, no. 3, March 1973, pp. 268-278.

[18] S.S.H. Wijayasuriya, G.H. Norton, J.P. McGeehan, "A Sliding Window Decorrelating Algorithm for DS-CDMA Receivers," *Electronics Letters*, vol. 28, no. 17, August, 1992, pp.1596-1598.

[19] G. Ungerboeck, "Adaptive Maximum-Likelihood Receiver for Carrier-Modulated Data-Transmission Systems," *IEEE Trans. on Comm.*, vol. 22, no. 5, May 1974, pp. 624-636.

[20] M. Kocic, D. Brady, "Asymptotic Multiuser Efficiency of the Maximum Likelihood Sequence Detector with Channel Mismatch," *Proceedings of CISS'93.*

[21] X. Zhang, D. Brady, "Soft-Decision Multistage Detectors for Asynchronous AWGN Channels," submitted to CTMC at GLOBECOM'93.

[22] S.D. Gray, D. Brady, "The Asymptotic Multiuser Efficiency of Two-Stage Detection in Mismatched AWGN Channels," submitted to CTMC at GLOBECOM'93.

[23] Z. Zvonar, D. Brady, "Multiuser Detection in Single-Path Fading Channels", to appear in *IEEE Trans. on Comm.*.

[24] Z. Xie, C.K. Rushforth, R.T. Short, "Multiuser Signal Detection Using Sequential Decoding," *IEEE Trans. on Comm.*, vol. 38, no. 5, May 1990, pp. 578-583.

[25] S. Verdu, "Recent Progress in Multiuser Detection," *Advances in Communications and Control Systems, ComCon '88*, Lecture Notes in Control and Information Science Series, NY, Springer-Verlag, 1989.

[26] J.G. Proakis, *Digital Communications*, New York: McGraw-Hill, 1983.

[27] P.R. Chevillat, E. Eleftheriou, "Decoding of Trellis-Encoded Signals in the Presence of Intersymbol Interference and Noise," *IEEE Trans. on Comm.*, vol. 37, no. 7, July 1989, pp. 669-676.

[28] K. Wesolowski, "Efficient Digital Receiver Structure for Trellis-Coded Signals Transmitted Through Channels With Intersymbol Interference," *Electronics Letters*, vol. 23. no. 24, November 1987, pp. 1265-1267.

[29] J. Hagenauer, P. Hoeher, "A Viterbi Algorithm with Soft-Decision Outputs and its Applications," *Proceedings of GLOBECOM '89*, Dallas, Texas, Nov. 1989, pp. 1680-1686.